CR 134561

COLUMBIA UNIVERSITY

SYSTEMS RESEARCH GROUP

DEPARTMENT OF
ELECTRICAL ENGINEERING
SCHOOL OF ENGINEERING AND
APPLIED SCIENCE
NEW YORK, N.Y. 10027

(NASA-CR-134561) PERIODICALLY SWITCHED LOSSLESS NETWORKS (Columbia Univ.) 130 p N74-71755

Unclas
00/99 31269

CR 134561

PERIODICALLY SWITCHED LOSSLESS NETWORKS

Mebenin Awipi

Technical Report No. 111

June 1969

Vincent R. Lalli
Project Manager
Lewis Research Center
Office of Reliability
& Quality Assurance
21000 Brookpark Rd
Cleveland, OH 44135

This work was supported in part by the National Aeronautics and Space Administration under Grant NGR-33-008-090 and by the National Science Foundation under Grant GK-2283.

ABSTRACT

This thesis reports the results of a study of a class of periodically time-varying lossless networks. These networks are made up of ideal inductors, capacitors, and switches, with the lossless condition achieved by simple topological constraints. A complete state-space solution is given for the subclass of networks which possess a proper tree for both positions of the switches and may be completely described by the same state vector in the two time intervals during which the network is time-invariant.

Time-varying system functions for switched lossless (SLC) networks may be defined in a manner analogous to the treatment of time-invariant lossless (LC) networks. Properties of such system functions, especially those derived from the lossless condition, lead to further analogies to, and extensions of, the frequency domain properties of LC networks.

Various frequency-power formulas derived herein and an efficiency relation deduced from them may be compared to those of nonlinear reactive and resistive elements. The comparison shows, in particular, that Page's inverse-square law of harmonic generation may be bypassed. The difference between the ideal switch and other switching devices such as the ideal diode and silicon controlled rectifiers thus may be clarified, and a possible circuit is given for simulating the ideal switch at large signal or power levels.

Finally, the problem of realizing the network functions of linear time-varying networks using only ideal switches as time-varying elements is considered briefly. For the fundamental case of the driving point admittance function of a lossless, periodically time-varying one-port network, a suitable network structure is selected and analyzed. This analysis shows that the poles of a given admittance function can be realized exactly, but the residue function, while appropriately periodic in time with the period of the network variation, cannot be arbitrarily specified. However, an exhaustive treatment of the design flexibility possible for the given scheme is not carried out due to the lack of comprehensive realizability conditions and tolerances for linear time-varying networks.

ACKNOWLEDGEMENT

The author takes great pleasure in acknowledging the guidance and support provided by Professors Henry E. Meadows and Thomas E. Stern, his advisors, during the course of research leading to this thesis.

The author is grateful to Professors William R. Bennett and Amiya K. Sen for their help throughout the period of his graduate studies at Columbia.

To my colleague, Julius Bola Oso, I am grateful for many hours of fruitful discussion. I also wish to express my appreciation to Alma Jean Chapman for her patience in typing several drafts of this thesis under rather trying circumstances.

The work reported herein was supported in part by the National Aeronautics and Space Administration under Grant NGR 33-008-090 and by the National Science Foundation under Grant GK-2283.

TABLE OF CONTENTS

(Cont.)

TABLE OF CONTENTS (Cont.)

PERIODICALLY SWITCHED LOSSLESS NETWORKS

CHAPTER 1: INTRODUCTION

1.1 Background of Problem

The study of Linear Time-Varying Networks and Systems as a branch of electrical engineering science may be regarded as a consequence of perturbation analyses of nonlinear systems. In parametrically excited linear systems or linearized versions of nonlinear systems in which a small signal is imposed on a large waveform, the equations describing input-output relations become linear ordinary differential equations with time-varying coefficients of the form

$$\sum_{n=0}^{N} a_n(t) \frac{d^n y}{dt^n} = \sum_{m=0}^{M} b_m(t) \frac{d^m u}{dt^m} \qquad (1)$$

where $u(t)$ is the input waveform, $y(t)$ is the response function and t represents the independent time variable. In particular, parametrically-excited circuits and systems have been extensively analyzed from this point of view, using the available mathematical theory for equations of type (1) to obtain information on stability bounds and the amplitudes and frequencies of sustained oscillations. The analyses employed at that stage still could properly be regarded as lying in the realm of applied mathematics.

About two decades ago, using as background and motivation the rapid development of linear time-invariant network theory, Darlington, Zadeh and others began to generalize concepts of this theory to the time-varying case. Thus integral transforms were defined, leading to time-varying versions of impedance and admittance functions, as well as various pole and residue concepts.

The general analyses[1,2] of linear time-varying networks postulate as circuit elements time-varying but usually positive definite resistances $R(t)$, capacitances $C(t)$ and inductances $L(t)$, and sometimes transformers of turns-ratio $T(t)$.[5] However, synthesis schemes[3] which lead from a given network description to a set of elements $\{R(t), C(t), L(t), T(t)\}$, their functional values, and a network configuration are not as readily available as in the time-invariant case, where the analysis and synthesis processes are comparatively straightforward algebraic processes. The available synthesis and modelling schemes usually employ constant RLCT elements and only one class of time-varying elements. For example, Spaulding and others,[5,6] postulate a time-varying, passive, lossless transformer for their synthesis schemes. In another approach[4], multipliers and a set of specially generated signals are postulated for use in a generalized n-path structure; the multipliers and generated signals function as time-varying amplifiers (which may be regarded as time-varying resistances if the inputs are currents and the outputs are voltages, and vice versa).

Another element which can be used as a time-varying element is the ideal switch. An ideal switch is postulated to have the following characteristics:

(1) It has zero resistance in the "closed" state and can conduct current in either direction.

(2) It has infinite resistance in the "open" state and can sustain voltages of either polarity across its terminals without conduction.

(3) It can be opened or closed instantaneously by applying an appropriate trigger waveform to a control terminal at instants independent of the orientation or magnitude of the voltages and currents at the other terminals.

While such an ideal switching device is not generally available as a single unit, it may be realized approximately from available components at various frequency ranges and power levels. A practically significant class of such components introduced in the last decade consists of silicon controlled rectifier (SCR) devices. These rugged devices have been applied widely in efficient and compact power processing circuits demanded for space-vehicle and satellite applications.[7,8,9] We thus have both theoretical and practical motivations for the study of the class of networks undertaken herein.

1.2 Statement of Problem

The central problem considered here is the mathematical characterization of networks of ideal capacitors, inductors and switches in which the inductances and capacitances are linear, positive and time-invariant, and the switches are opened and closed periodically, thus providing a linear, passive periodically time-varying system. By imposing simple topological constraints, we avoid the possibility of instantaneous charge or flux transfer, so that the switches operate without loss of energy. The networks concerned then may be referred to as switched lossless (SLC) networks, a generalization of the classical time-invariant lossless (LC) networks treated by Foster, Cauer, Darlington and others. The class of SLC networks includes many circuits that have been used in frequency conversion and power processing systems, but no general analysis of their behavior has been available. Moreover, general analyses of switched networks have not dealt specifically with this important subclass of networks, since they usually rely on assumptions of asymptotic stability. It is the purpose of the research presented here to provide a general analysis of the class of SLC networks, exploiting the analogy between SLC and LC networks, and relating the results obtained, in particular, to frequency conversion networks.

1.3 Historical Review

Since periodically switched networks form a subclass of the general class of linear networks with time-variable elements, most of the results of the general theory of networks of the latter type are directly applicable to switched networks. For example, Floquet's theorem is valid and time-variable system functions of the type introduced by Zadah may be defined. Modern analysis of periodically time-varying networks and systems usually start with the state-space equations in the normal form

$$\dot{x}(t) = A(t)x(t) + B(t)u(t) \tag{2}$$

where the n-square matrix A(t) and the n-column vector B(t) are periodic in time t and continuously differentiable to any order desired. For switched networks, A(t) and B(t) are piecewise constant between switching intervals and discontinuous at the switching instants. Because of the discontinuity of the coefficients, extensive manipulations of the state equation (2) which usually involve differentiation of the coefficients are difficult or not possible. However, the piecewise constant nature of the coefficients permits some simplifications in actually obtaining a solution of the equation and most of the effort is then directed to exploiting the solution.

The first general analysis of switched networks was published by Bennett[10] in 1955; he used classical transform techniques to calculate the time-domain response in successive time intervals corresponding to alternate states of a switch. The two solutions at each instant of change of state were matched by setting the final values of inductor currents and capacitor voltages in one interval equal to the initial values of those quantities in the succeeding interval. In 1958, following the introduction of Bashkow's A-matrix into network theory, Desoer[11] presented an analysis similar to Bennett's in principle, but utilizing the state-space formulation and matrix operations. The solutions of both the transient and steady-state problems were expressed in a compact form suitable for automatic computation. It may be noted that both Bennett and Desoer used the assumption of continuity of the state-vector (made up of certain inductor currents and capacitor voltages), which is mathematically convenient in obtaining closed form solutions valid for all positive time, but did not stress its physical significance as the condition for lossless operation. Their work was motivated by small-signal processing circuits in time-domain multiplex systems where signals may be amplified after processing; whereas for power-processing applications, lossless operation becomes a matter of prime importance.

Significant but specialized analytical work suitable for particular applications was done by Fettweis[12] on frequency converters, by Fischl and others[13-17] on commutated networks, and by several authors[18-21] on synchronous networks used for compensation of suppressed-carrier control systems. In cases where specific networks were considered, they were all networks of switches, resistors and capacitors because the main objective of many of these efforts was to obtain band-pass characteristics without the use of inductors (either because inductance cannot be realized directly in integrated circuits or because the required size or quality of inductors is prohibitive).

In addition, two approximate analyses of the resonant transfer filter used in time-multiplex communication systems were performed by Desoer[22] and Ozone[23]. The efforts of several authors to improve the conversion efficiency of ring modulators had also involved some work on simple networks with switches and filters.[24-27]

More recently, Sun[28] and Sun and Frisch[29] have generalized Desoer's approach to include nonsynchronous operation of the switches and to give a unified treatment of commutated and synchronous networks using the state-variable formulation, while Liou and Mastromonaco[30] have treated the case of discontinuous state-vectors by defining coupling matrices at the switching instants, and presented an exact analysis of the resonant transfer filter.

The state-space formulation presented in Chapter 2, which serves as the starting point in the mathematical characterization of SLC networks, parallels the technique developed by Bennett[10], Desoer[11], and Sun.[28] However, the results presented in this report go further in examining significant aspects of the solution and relating the characterization thus derived to the physical properties and applications of the networks.

1.4 Outline of Thesis

The organization of the rest of the thesis is as follows:

In Chapter 2, we present the state-space formulation and solution of the equations of SLC networks. Section 2.1 discusses the topological constraints to be satisfied for lossless operation of the switches and gives possible canonical structures for 2-port SLC networks. Section 2.2 presents the state-space analysis for the restricted case where the SLC networks are of the canonical types, while Section 2.3 considers the general SLC networks. In Section 2.4, a summary of formulas is given to facilitate computational procedure and a simple SLC network is analyzed to illustrate some aspects of the procedure.

In Chapter 3, relevant aspects of the state-space solution are examined further, leading to the definition of time-varying system functions for SLC networks. Properties of the system functions similar to those of lumped linear time-varying networks are discussed and properties of the system functions for 1-port and 2-port networks are developed as consequences of the lossless condition.

Chapter 4 deals with frequency-power formulas and some practical aspects of SLC networks. The real-power formulas are contrasted with those of nonlinear reactive and resistive elements, and the possibility of bypassing Page's inverse-square law in harmonic generation efficiency using SLC networks is demonstrated. In this context, the position of the ideal switch among "switching" elements is discussed and a possible circuit for simulating the ideal switch at reasonable power levels and frequency ranges is given.

Chapter 5 discusses the possibility of designing and modelling linear time-varying systems and networks using only ideal switches as time-varying elements. Although the general commutated n-path network may be used to simulate the state-equations, a more tractable scheme for input-output system function design is shown to be a parallel or cascade set of basic 2-path networks analogous to the Cauer partial fraction synthesis of LC networks.

Chapter 6 gives a summary of results and suggestions for further research.

References for Chapter 1

1. Darlington, S., "An Introduction to Time-Variable Networks," Proc. of the Midwest Symposium on Circuit Analysis, Univ. of Illinois, 1955, pp. 5-1 to 5-25.

2. Zadeh, L. A., "Frequency Analysis of Variable Networks," Proc. IRE, Vol. 38, March 1950, pp. 291-299.

3. Cruz, J. B. and Van Valkenburg, M. E., "The Synthesis of Models for Time-Varying Linear Systems," Proc. of the Symp. on Active Networks and Feedback Systems, Polytechnic Inst. of Brooklyn, April 1960, pp. 527-544.

4. Meadows, H. E., Silverman, L. M. and Franks, L. E., "A Canonical Network for Periodically Variable Linear Systems," Proc. of the Allerton Conf. on Circuit and System Theory, Vol. 4, pp. 649-658; 1966.

5. Spaulding, D. A., "Passive Time-Varying Networks," Ph.D. dissertation, Stanford University, Stanford, Calif., Jan. 1965.

6. Anderson, B. D., Spaulding, D. A. and Newcomb, R. W., "The Time-Variable Transformer," Proc. IEEE, Vol. 53, June 1965, p. 634.

7. Hartman, D. J., et alia: "Adaptive Power Conditioning for Solar Cell Arrays," Sup. to IEEE Trans. on Aerospace and Electronic Systems, Vol. AES-2, No. 6, Nov. 1966, pp. 43-47.

8. Bedford, B. D. and Hoft, R. F., Principles of Inverter Circuits; New York: John Wiley and Sons, 1964.

9. Gentry, F. E., et alia, Semiconductor Controlled Rectifiers: Principles and Applications of p-n-p-n Devices, Englewood Cliffs, N.J.; Prentice Hall, 1964.

10. Bennett, W. R., "Steady State Transmission Through Networks Containing Periodically Operated Switches," IRE Trans. on Circuit Theory, Vol. CT-2, pp. 17-21, March 1955.

11. Desoer, C. A., "Transmission Through a Linear Network Containing a Periodically Operated Switch," WESCON Convention Record, pt. 2, Circuit Theory, pp. 34-41, 1958.

12. Fettweis, A., "Steady-State Analysis of Circuits Containing a Periodically Operated Switch," IRE Trans. on Circuit Theory, Vol. CT-6, pp. 252-260, Sept. 1959.

13. Fischl, R., "Analysis of a Commutated Network," IEEE Trans. on Aerospace and Navigational Electronics," pp. 114-123, June 1963.

14. Acampara, A., Rabinovici, B. and Renton, C. A., "Generation of Bandpass Filters by Switching Techniques," Proc. IEEE, Vol. 51, pp. 256-257, Jan. 1963.

15. Franks, L. E. and Sandberg, I. W., "An Alternate Approach to the Realization of Network Transfer Functions: The n-Path Filter," Bell Sys. Tech. J., Vol. 39, pp. 1321-50, Sept. 1960.

16. Smith, B. D., "Analysis of Commutated Networks," IRE Trans. PGAE-10, pp. 21-26, Dec. 1953.

17. LePage, W. R., Cahn, C. R. and Brown, J. S., "Analysis of a Comb Filter Using Synchronously Commutated Capacitors," AIEE Trans., pt. 1, Vol. 72, pp. 63-68, March 1953.

18. Weiss, G., "Synchronous Networks," IRE Trans. on Automatic Control, Vol. AC-7, pp. 45-54, March 1962.

19. Bohn, E. V., "A Simple Method for the Analysis of Demodulator Compensating Networks," IRE Trans. on Circuit Theory, Vol. CT-8, pp. 306-311, Sept. 1961.

20. Knox, A. and Murphy, G. J., "Method for the Design of Phase Lead Demodulating Compensators for Use in Carrier Control Systems," IEEE Trans. on Automatic Control, Vol. AC-8, pp. 333-338, Oct. 1963.

21. Bolier, V. W., "Analysis of a Special Purpose RC Filter Incorporating a Periodically Conducting Bilinear Element," IRE Proc., Vol. 42, No. 9, pp. 1435-1438, Sept. 1954.

22. Desoer, C. A., "A Network Containing a Periodically Operated Switch Solved by Successive Approximation," Bell Syst. Tech. J., Vol. 36, pp. 1403-1428, Nov. 1957.

23. Ozone, K., "An Approximate Analysis of a Periodically Switched Filter," IEEE Trans. on Comm. Tech., Vol. Com-15, No. 2, pp. 163-168, April 1967.

24. Belevitch, V., "Linear Theory of Bridge and Ring Modulator Circuits," Electrical Communication, Vol. 25, No. 1, pp. 62-73, 1948.

25. Tucker, D. G., "Rectifier Modulators with Frequency-Selective Terminations," Proc. IEE (London), Vol. 96, pt. 3, No. 43, pp. 422-428, Sept. 1949.

26. Belevitch, V., "Effect of Rectifier Capacitances on the Conversion Loss of Ring Modulators," IRE Trans. on Circuit Theory, Vol. Ct-2, pp. 41-44, March 1955.

27. Kurth, C., "Analysis of Diode Modulators Having Frequency-Selective Terminations Using Computers," Electrical Communication, Vol. 39, No. 3, pp. 369-378, 1964.

28. Sun, Y., "Networks Containing Periodic Switches: A Unified Approach and Applications," Ph.D. Thesis, Dept. of Electrical Engineering and Computer Sciences, Univ. of California, Berkeley, September 1967.

29. Sun, Y. and Frisch, I. T., "Transfer Functions and Stability for Networks with Periodically-Varying Switches," Proc. First Asilomar Conf. on Circuits and Systems.

30. Liou, M. L. and Mastromonaco, F. R., "Exact Analysis of Linear Circuits Containing a Periodically Operated Switch Using the State Space Approach," IEEE International Symposium on Circuit Theory, Miami Beach, Fla., Dec. 1968.

CHAPTER 2: STATE-SPACE ANALYSIS OF SLC NETWORKS

The objective of this chapter is to present the basic state-space formulation which is the starting point in the mathematical characterization of SLC networks developed later. In Section 2.1, we discuss the types of constraints necessary for the lossless operation of the switches in an SLC network. Also, other desirable features of an SLC network are noted and networks possessing these additional features are referred to as "canonical." Then in Section 2.2, the solution of the normal form state equations of SLC networks of the canonical types is presented, while Section 2.3 discusses the extension of the analysis to general SLC networks not constrained as in the previous section. A collection of the response equations of the canonical networks and an illustrative example are given in Section 2.4.

2.1 Topological Constraints and Canonical SLC Networks

To obtain the condition of losslessness in networks of ideal inductors, capacitors, and switches, we must arrange to avoid instantaneous charge transfer among capacitors or instantaneous flux transfer among inductors when switches are closed or opened. The potentially lossy situations are those obtaining when:

(1) by closing a switch we form an all-capacitive loopset and

(2) by opening a switch, we form an all-inductive cutset.

The simple cases of one or two reactive elements and a switch are shown in Fig. 2-1. For the case shown as (a) in the figure, if

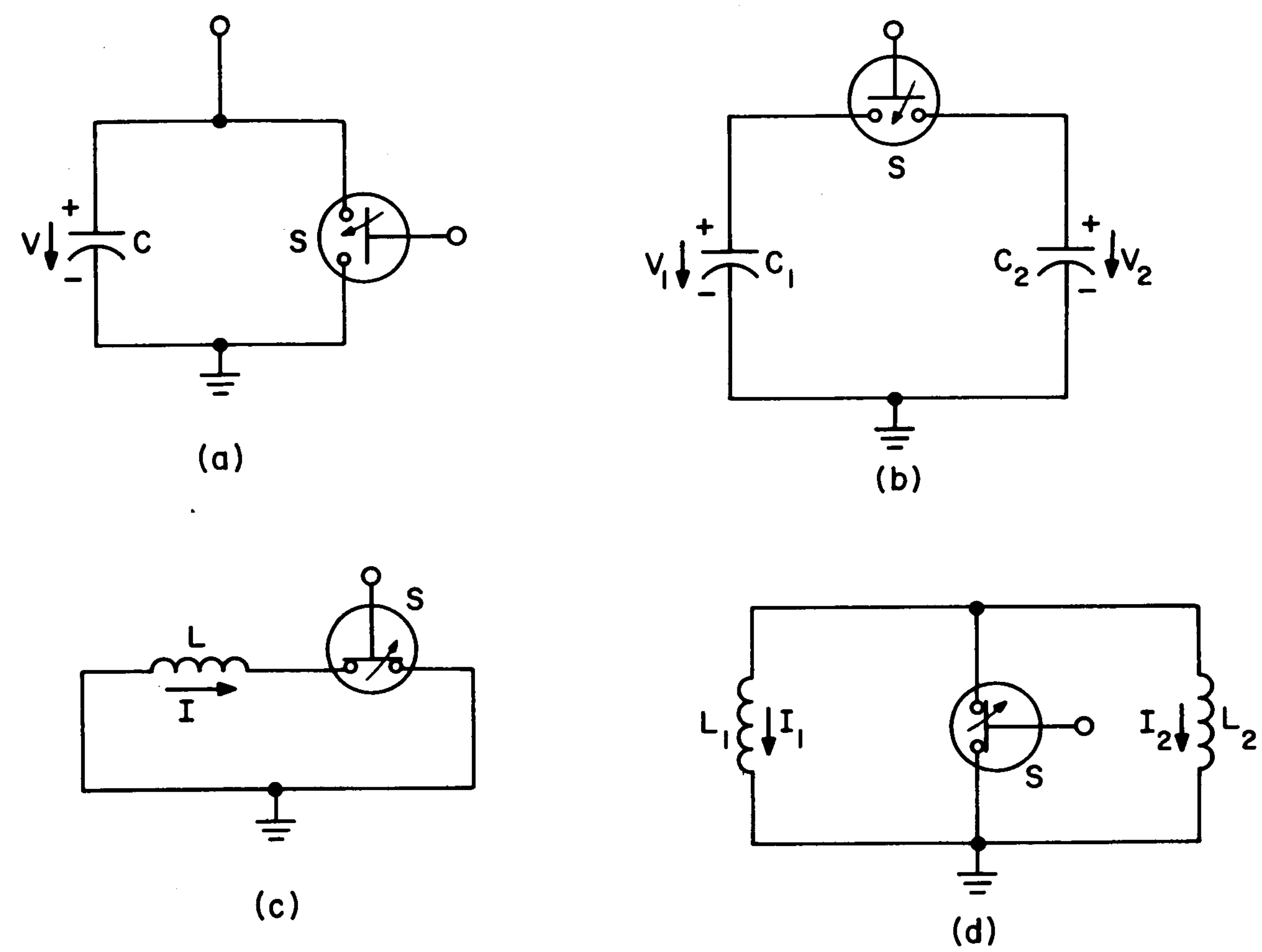

FIG. 2.1 POTENTIALLY LOSSY CONFIGURATIONS

the capacitor voltage is V just before the switch is closed, the energy lost is $E_1 = 1/2\ CV^2$, while for the case (b), if the voltages across capacitors C_1, C_2 are V_1, V_2 just before closure of the switch, the energy lost is

$$E_2 = \frac{1}{2} \frac{C_1 C_2}{C_1+C_2} (V_1-V_2)^2 .$$

In both cases the energy lost would be zero if a sensing mechanism were employed to close the switch only at instants when $V = 0$ in case (a) and only when $V_1 = V_2$ in case (b). However, apart from the additional complication introduced by such sensing devices, the switches could not be operated periodically in this mode, since, in general, the voltages in the network are not periodic. Hence, the more convenient manner of avoiding loss at switching instants is to disallow the potentially lossy configurations.

Cases (c) and (d) of the figure are the duals of the first two cases.

Although there is an uncountable number of SLC networks constrained as above, yet for the benefit of the analysis in the next section, we shall define possible canonical SLC networks by picking certain canonical LC networks and inserting switches at appropriate points in the configuration such that the switches could be operated

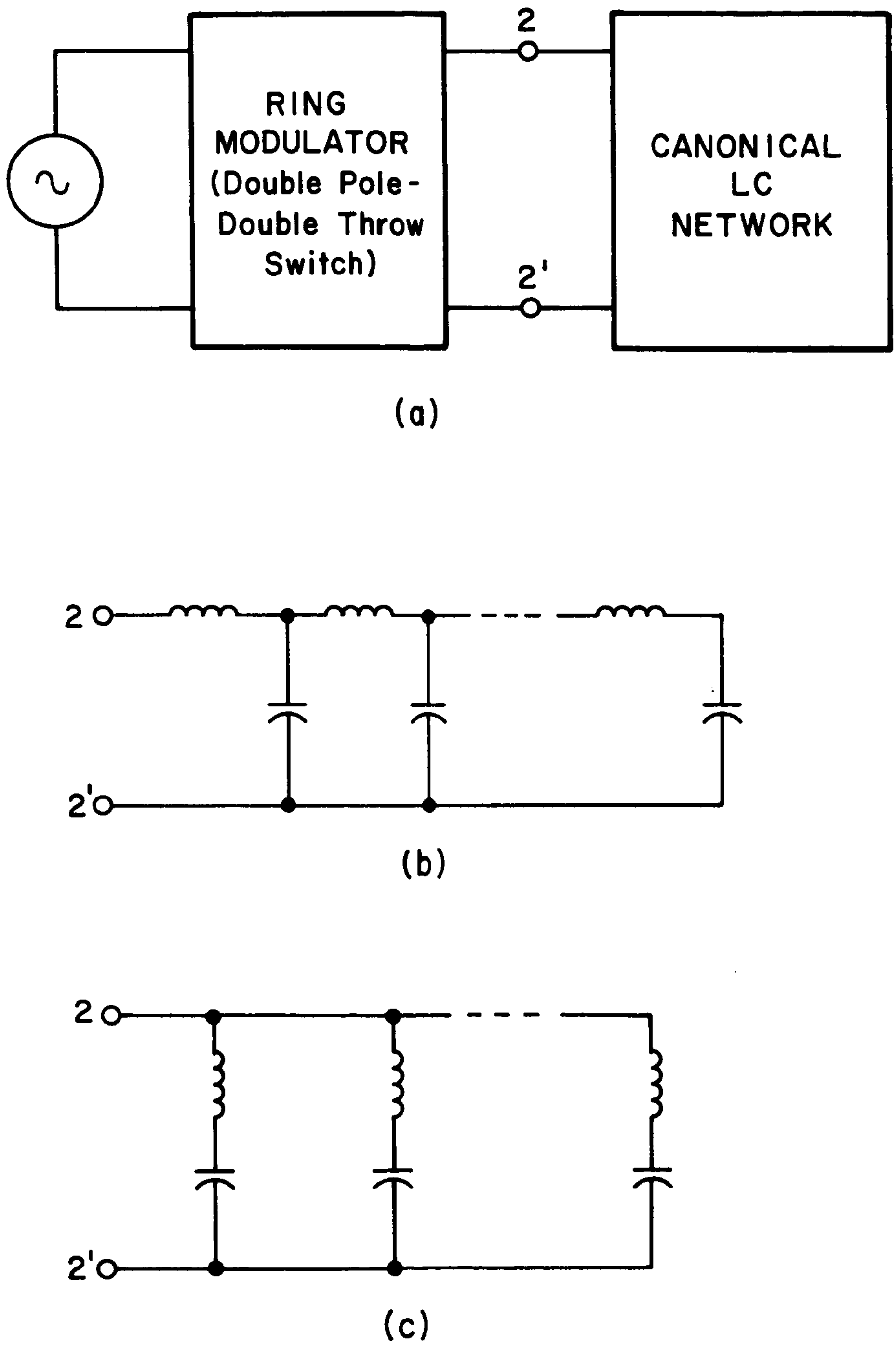

FIG. 2.2 CANONICAL SLC 1-PORT NETWORKS

periodically without loss. To simplify the state-space formulation, we choose LC networks with proper trees so that every capacitor is in a tree and every inductor in the co-tree. Then the state vector consisting of the set of inductor currents and capacitor voltages completely describes the network variables at all times.

SLC networks satisfying the canonical conditions are shown in Figs. 2-2 and 2-3. These canonical forms are useful for theoretical illustrations and, in some cases, are extensions of simple cases which have been in practical use. However, in practice, a single switch is usually sufficient for obtaining the desired switched characteristics.

If an ideal current source is the type of excitation desired, we may use the duals of the circuits shown.

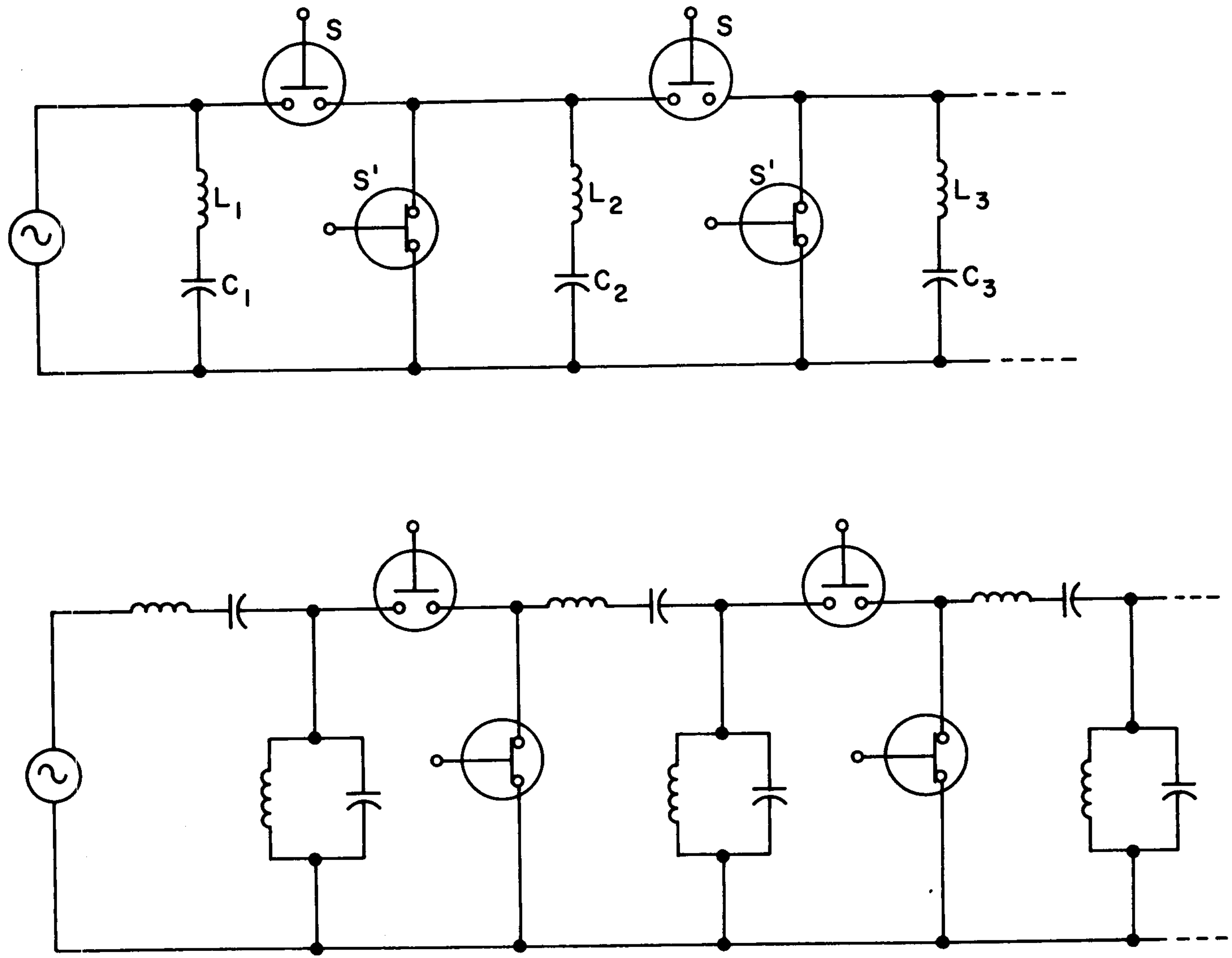

FIG. 2.3 OTHER FORMS OF CANONICAL SLC NETWORKS

2.2 State-Space Formulation

Consider an SLC network driven by a source e^{pt}. Assume that there are two time intervals I_{1k} and I_{2k} in which the state-matrices are constant, i.e., either there is only a single switch or the several switches of the network are operated synchronously. Suppose also, as discussed in the preceding section, that the same state variables completely describe the network in each time interval. Then we can write the normal form equations of the network in the following manner:

$$\dot{x} = A_1 x + B_1 e^{pt}\ , \ t \in I_{1k} : kT<t<kT+T_1 \tag{1a}$$

$$\dot{x} = A_2 x + B_2 e^{pt}\ , \ t \in I_{2k} : kT+T_1<t<(k+1)T \tag{1b}$$

where:

A_1 and A_2 are constant real square matrices of order n , say

B_1 and B_2 are constant nx1 column vectors

k is an integer

T is the switching period

$T_{1/T}$ is the duty cycle of the switch.

I_{1k} and I_{2k} represent time intervals and

x represents the state vector.

Making a change of variables for convenience,

$$Z(t) = x(t)e^{-pt} \tag{2a}$$

we obtain equations for $Z(t)$ as

$$Z = E_1 Z + B_1 \ , \ t \in I_{1k} \tag{2b}$$

$$Z = E_2 Z + B_2 \ , \ t \in I_{2k} \tag{2c}$$

where

$$E_1 = A_1 - pI \tag{3a}$$

$$E_2 = A_2 - pI \tag{3b}$$

and I is the unit square matrix of order n.

Let

$$Z_{1k}(t) = Z(t) \ , \ t \in I_{1k}$$

$$Z_{2k}(t) = Z(t) \ , \ t \ E \ I_{2k}$$

as illustrated in Fig. 2-4. Then we obtain the following solutions for $Z(t)$ from (2b) and (2c).

$$Z_{1k}(t) = e^{E_1(t-kT)} Z(kT) + \left[e^{E_1(t-kT)} - I \right] E_1^{-1} B_1 \tag{4a}$$

$$Z_{2k}(t) = e^{E_2(t-kT-T_1)} Z(kT+T_1) + \left[e^{E_2(t-kT-T_1)} - I \right] E_2^{-1} B_2 \tag{4b}$$

Because of the constraint of lossless switching and the assumption that the state vector consists of capacitor voltages and inductor currents, the values of $x(t)$, and hence $Z(t)$, are continuous at the switching instants; thus

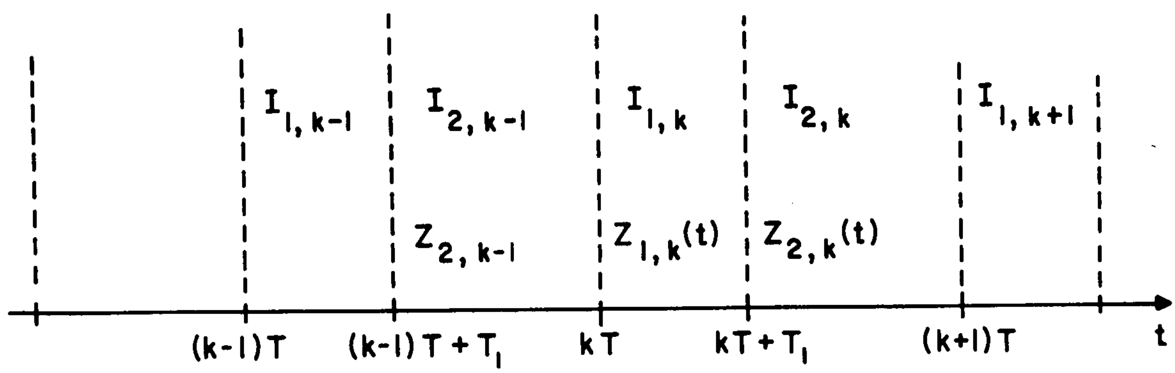

FIG. 2.4 SWITCHING TIME INTERVALS

$$Z_{1,k+1}(kT+T) = Z_{2,k}(kT+T) = Z(kT+T) \tag{5a}$$

$$Z_{1k}(kT+T_1) = Z_{2k}(kT+T_1) = Z(kT+T_1) \tag{5b}$$

From (4a)

$$Z(kT+T_1) = e^{E_1T_1} Z(kT) + \left[e^{E_1T_1}-1\right] E_1^{-1}B_1 \tag{6a}$$

and from (4b)

$$Z(kT+T) = e^{E_2T_2} Z(kT+T_1) + \left[e^{E_2T_2}-I\right] E_2^{-1}B_2 \tag{6b}$$

Eliminating $Z(kT+T_1)$ from (6a) and (6b), yields

$$Z(kT+T) = QZ(kT) + G \tag{7}$$

where matrix Q and vector G are defined as follows. Let

$$Q_1 = e^{E_1T_1}, \quad Q_2 = e^{E_2T_2} = e^{E_2(T-T_1)} \tag{8a}$$

$$G_1 = (Q_1-I)\ E_1^{-1}B_1 \tag{8b}$$

$$G_2 = (Q_2-I)\ E_1^{-1}B_1 \tag{8c}$$

Then

$$Q = Q_2Q_1 \tag{8d}$$

$$G = Q_2G_1 + G_2 \tag{8e}$$

The difference equation (7) has the solution

$$Z(kT) = Q^kZ_0 + (I-Q^k)(I-Q)^{-1}\ G \tag{9a}$$

so that $Z(kT+T_1) = Q_1Z(kT) + G_1$. (9b)

From (2a), (4) and (9), we may now write expressions for the state vector $x(t)$ as

$$x(t) = \begin{cases} e^{E_1(t-kT)}\left[Z(kT)+E_1^{-1}B_1\right]e^{pt} - E_1^{-1}B_1e^{pt}\ , & t \in I_{1k} \qquad (10a) \\ e^{E_2(t-kT-T_1)}\left[Z(kT+T_1)+E_2^{-1}B_2\right]e^{pt} - E_2^{-1}B_2e^{pt}\ , & t \in I_{2k} \qquad (10b) \end{cases}$$

Equation (10) provides a complete solution for the state-variable response of the network in terms of the initial conditions and the coefficient matrices in normal form description (1).

2.3 Extension to General SLC Networks

The analysis presented above represents the simplest and most restricted form of the state-space formulation of switched networks. Several extensions are possible and have been treated in the literature. Sun[1] has treated the case in which the switches are not necessarily operated in synchronism, but where all switches are operated with the same period T, so that the basic time interval $kT<t<kT+T$ is, in general, divided into n subintervals I_{ik} during which the state-matrices are constant. Liou and Mastromonaco[2] have recently dealt with the case where the state-vectors may be different in the different subintervals and discontinuous at the switching instants. In their work, coupling matrices are used to relate adjacent state vectors at the switching instants to enable a continuation of the solution over all positive time.

For SLC networks, the most general case of interest is that where the state vectors consist of ambit charges and loop fluxes and not necessarily of individual capacitor voltages and inductor currents as previously assumed.[3,4] In this case, the state vectors may differ in different time intervals and so may be discontinuous at the switching intervals. However, as long as the network is lossless, there is a physical set of variables, consisting of individual capacitor voltages and inductor currents, which is invariant from one interval to the other and is continuous at the switching instants. The relation between the mathematically chosen state vectors $\{x_1,x_2\}$ and this physical vector $\{y\}$ may be written as

$$x_1 = S_1 y \tag{11a}$$

$$x_2 = S_2 y \tag{11b}$$

where:

y is a vector of order n

x_1, x_2, are vectors of order m, $m \leq n$

The matrices S_1 and S_2 express the fact that in the general case, the state vectors are linear combinations of the capacitor voltages and inductor currents, in contrast to the case of the canonical SLC networks in which the state vector is simply the set of all capacitor voltages and inductor currents. However, since for lossless operation of the switches, the same all-capacitive loopsets and all inductive cutsets must be present in both time intervals, a unique relation exists between the vectors x_1 and x_2:

$$x_1 = C x_2 \tag{11c}$$

where

C is a constant nonsingular matrix of order $m \times m$.

The normal form equations of the general SLC network may then be written as:

$$\dot{x}_1 = A_1 x_1 + B_1 e^{pt} \tag{12a}$$

$$\dot{x}_2 = A_2 x_2 + B_2 e^{pt} \tag{12b}$$

with the change of dependent variables

$$Z_i = x_i e^{-pt} \text{ , } W = ye^{-pt} \text{ , } i = 1,2$$

we have

$$\dot{Z}_1 = E_1 Z_1(t) + B_1 \ , \ Z_1(t) = S_1 W(t) \ , \ t \in I_{1k} \tag{13a}$$

$$\dot{Z}_2 = E_2 Z_2(t) + B_2 \ , \ Z_2(t) = S_2 W(t) \ , \ t \in I_{2k} \tag{13b}$$

The solution of (13) is

$$Z_1(t) = e^{E_1(t-kT)} Z_1(kT) + \left[e^{E_1(t-kT)} - I \right] E_1^{-1} B_1 \ , \ t \in I_{1k} \tag{14}$$

$$Z_2(t) = e^{E_2(t-kT-T_1)} Z_2(kT+T_1) + \left[e^{E_2(t-kT-T_1)} - I \right] E_2^{-1} B_2 \ , \ t \in I_{2k} \tag{15}$$

The boundary conditions at the switching instants are

$$S_1 W(kT+T_1) = Z_1(kT+T_1) = CZ_2(kT+T_1) \tag{16a}$$

$$S_2 W(kT+T) = Z_2(kT+T) = C^{-1} Z_1(kT+T) \tag{16b}$$

From (14) and (15) we have

$$Z_1(kT+T_1) = Q_1 Z_1(kT) + G_1 \tag{17a}$$

$$Z_2(kT+T) = Q_2 Z_2(kT+T_1) + G_2 \tag{17b}$$

Hence from (16) and (17) we obtain

$$Z_1(kT+T) = QZ_1(kT) + G \tag{18}$$

where the new quantities Q and G are defined as

$$Q = CQ_2 C^{-1} Q_1 \tag{19}$$

$$G = CQ_2 C^{-1} G_1 + CG_2 \tag{20}$$

The solution of equation (18) is again

$$Z_1(kT) = Q^k Zo + (I-Q^k)(I-Q)^{-1} G \tag{21}$$

The sequence of equations (21), (17), (16), (15) and (14) constitute the complete solution of the system (12).

2.4 Summary of Response Equations for Canonical Case

We summarize below the scattered expressions and definitions leading to equation (10) for easy reference. Then we shall make a few calculations on a relatively simple circuit to illustrate the use of the summary of formulas.

For the system (1):

$$E_1 = A_1 - pI \ , \ E_2 = A_2 - pI \tag{3}$$

$$\left.\begin{aligned}
Q_1 &= e^{E_1T_1} = e^{-pT_1} e^{A_1T_1} \\
Q_2 &= e^{E_2T_2} = e^{-p(T-T_1)} e^{A_2(T-T_1)} \\
Q &= Q_2Q_1 = e^{-pT} e^{A_2(T-T_1)} e^{A_1T_1} \\
G_1 &= (Q_1 - I)\, E_1^{-1}B_1 = (I-Q_1)(pI-A_1)^{-1}B_1 \\
G_2 &= (Q_2 - I)\, E_2^{-1}B_2 = (I-Q_2)(pI-A_2)^{-1}B_2 \\
G &= Q_2G_1 + G_2
\end{aligned}\right\} \tag{8}$$

$$\left.\begin{aligned}
Z(kT) &= Q^k Z_o + (I-Q^k)(I-Q)^{-1}G \\
Z(kT+T_1) &= Q_1 Z(kT) + G_1
\end{aligned}\right\} \tag{9}$$

$$x(t) = \begin{cases} e^{E_1(t-kT)} \left[Z(kT)+E_1^{-1}B_1\right] e^{pt} - E_1^{-1}B_1 e^{pt} \ , & t \in I_{1k} \\ e^{E_2(t-kT-T_1)} \left[Z(kT+T_1) + E_2^{-1}B_2\right] e^{pt} - E_2^{-1}B_2 e^{pt} \ , & t \in I_{2k} \end{cases} \tag{10}$$

Example: To illustrate the use of the summary of response equations in a systematic computation of the response of an SLC network to an exponential input e^{pt}, let us consider the generalized series-capacitor inverter circuit shown in Fig. 2-5. For the special case in which the input is a d-c voltage source (p=0) and the common switching frequency of the complementary switches S and S' is equal to the center frequency of the series RLC circuit, ($\omega_s=\beta$), this circuit is used as a d-c to a-c inverter with the voltage across the resistor as the output.[5]

Assume that in the time interval I_{1k}, S is closed and S' open and in I_{2k}, S is open and S' closed. Then the state vector is

$$\underset{\sim}{x} = \begin{bmatrix} v \\ i \end{bmatrix}$$

and the coefficients of the normal form state equations are

$$A_1 = A_2 = \begin{bmatrix} 0 & 1/C \\ -1/L & -R/L \end{bmatrix}$$

$$B_1 = \begin{bmatrix} 0 \\ 1/L \end{bmatrix}, \quad B_2 = \begin{bmatrix} 0 \\ 0 \end{bmatrix}.$$

Let $$\alpha = \frac{R}{2L}, \quad \beta^2 = \frac{1}{LC} - \frac{R^2}{4L^2}$$

Then $$(pI-A)^{-1} = \frac{1}{D(p)} \begin{bmatrix} p & 1/C \\ -1/L & p+2\alpha \end{bmatrix}$$

where $$D(p) - (p+\alpha)^2 + \beta^2.$$

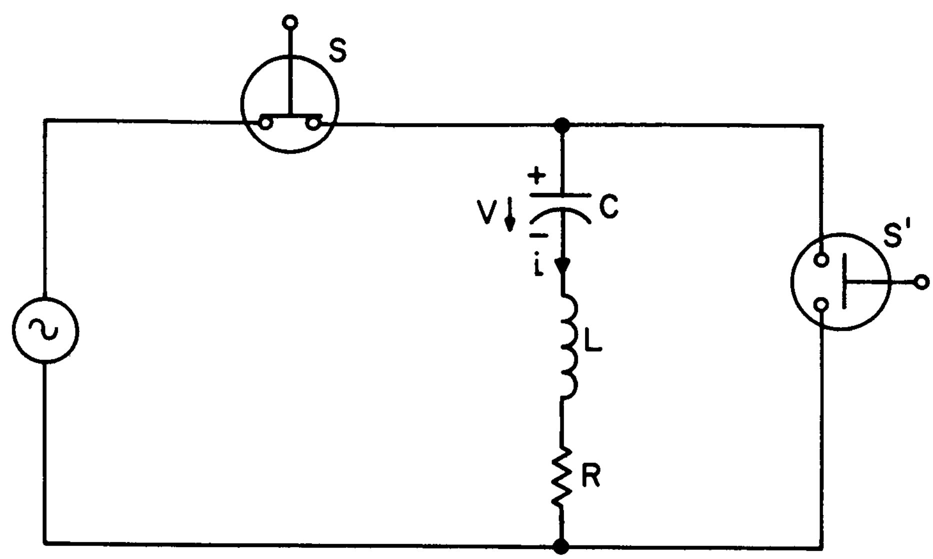

FIG. 2.5 SERIES-CAPACITOR INVERTER

Then the Q-matrices and G-vectors may be calculated from (8) as:

$$Q_i = e^{-(p+\alpha)T_i} \begin{bmatrix} \text{Cos } \beta \text{ } T_i - \frac{\alpha}{\beta} \text{ Sin } \beta \text{ } T_i & \frac{1}{\beta C} \text{ Sin } \beta \text{ } T_i \\ -\frac{1}{\beta L} \text{ Sin } \beta \text{ } T_i & \text{Cos } \beta \text{ } T_i + \frac{\alpha}{\beta} \text{ Sin } \beta \text{ } T_i \end{bmatrix}$$

$$G_1 = (I-Q_1)(pI-A_1)^{-1}B_1 = \begin{bmatrix} g_{11}(p) \\ g_{12}(p) \end{bmatrix}$$

where

$$g_{11}(p) = \frac{}{LC \cdot D(p)} \left[1 - e^{-(p+\alpha)T_1} \left\{ \text{Cos } \beta \text{ } T_1 + \frac{p+\alpha}{\beta} \text{ Sin } \beta \text{ } T_1 \right\} \right]$$

$$g_{12}(p) = \frac{1}{L \cdot D(p)} \left[p+2\alpha - e^{-(p+\alpha)T_1} \left\{ (p+2\alpha) \text{ Cos } \beta T_1 + \left(\frac{p+2\alpha+\frac{1}{LC}}{\beta} \right) \text{ Sin } \beta \text{ } T_1 \right\} \right]$$

$$G_2 = \begin{bmatrix} 0 \\ 0 \end{bmatrix} \quad \text{since} \quad B_2 = \begin{bmatrix} 0 \\ 0 \end{bmatrix}$$

$$G = Q_2 G_1 = \begin{bmatrix} g_1(p) \\ g_2(p) \end{bmatrix} \quad \text{where}$$

$$g_1(p) = g_{11}(p) e^{-(p+\alpha)T_2} \left[\text{Cos } \beta \text{ } T_2 - \frac{\alpha}{\beta} \text{ Sin } \beta T_2 \right] + \frac{g_{12}(p)}{\beta C} e^{-(p+\alpha)T_2} \text{Sin } \beta \text{ } T_2$$

$$g_2(p) = -\frac{1}{\beta L} g_{11}(p) e^{-(p+\alpha)T_2} \text{ Sin } \beta T_2 + g_{12}(p) e^{-(p+\alpha)T_2} \left[\text{Cos } \beta \text{ } T_2 + \frac{\alpha}{\beta} \text{Sin } \beta \text{ } T_2 \right].$$

The vectors $z(kT)$ and $z(kT+T_1)$ may next be calculated from (9) and the complete state response obtained from (10). However, the algebraic expressions become increasingly unwieldy, so that we shall not continue the computation any further for a general input e^{pt}.

For the special case of inverter operation, the input is d-c so that $p = 0$, and letting $T_1 = T_2 = \frac{1}{2}T$ and $\beta T = 2\pi(2n+1)$, we obtain

$$Q_1 = Q_2 = -e^{-\alpha T/2}\, I$$

$$Q = e^{-\alpha T}\, I$$

$$G_1 = \left(1+e^{-\alpha T/2}\right)\begin{bmatrix} 1 \\ 2\alpha C \end{bmatrix}, \quad G_2 = \begin{bmatrix} 0 \\ 0 \end{bmatrix}$$

$$G = -e^{-\alpha T/2}\left(1+e^{-\alpha T/2}\right)\begin{bmatrix} 1 \\ 2\alpha C \end{bmatrix}.$$

In the steady state, as discussed later in Chapter 3,

$$Z(kT) = (I-Q)^{-1}G = \frac{-e^{-\alpha T/2}\left(1+e^{-\alpha T/2}\right)}{1-e^{-\alpha T}}\begin{bmatrix} 1 \\ 2\alpha C \end{bmatrix}$$

$$Z(kT+T/2) = Q_1 Z(kT) + G_1$$

$$= \frac{1+e^{-\alpha T/2}}{1-e^{-\alpha T}}\begin{bmatrix} 1 \\ 2\alpha C \end{bmatrix}.$$

Taking the inductor current as the output, we have the solution

$$i(t) = \begin{cases} 2\alpha C + Y_{01}\, e^{-\alpha t_{1k}} \left[2\alpha C \operatorname{Cos} \beta t_{1k} + \left(\frac{2\alpha^2 C}{\beta} - \frac{1}{\beta L} \right) \operatorname{Sin} \beta t_{1k} \right] \\ \\ Y_{02}\, e^{-\alpha t_{2k}} \left[2\alpha C \operatorname{Cos} \beta\, t_{2k} + \left(\frac{2\alpha^2 C}{\beta} - \frac{1}{\beta L} \right) \operatorname{Sin} \beta t_{2k} \right] \end{cases}$$

where $t_{1k} = t\text{-}kT$, $t_{2k} = t\text{-}kT\text{-}T_1$

$$Y_{01} = \frac{-e^{-\alpha T/2}\left(1+e^{-\alpha T/2}\right)}{1-e^{-\alpha T}}$$

$$Y_{02} = \frac{1+e^{-T/2}}{1-e^{-\alpha T}} \quad .$$

It may be noted that for the practical inverter circuit in which

$$\beta = \omega_s \ ,$$

the switches need to conduct current in only one direction, so that generally available unidirectional switching devices such as silicon controlled rectifiers can be used in realizing the circuit. In general, with properly specified relations between the signal and switching frequencies, and the natural frequencies of the network, the state-space analysis presented in this chapter is valid for circuits using only such unidirectional switching devices in place of the ideal switch. Hence the response equations obtained here may be applied to the analysis of all commonly used power processing circuits. One of the consequences of postulating the ideal switch, however, is the theoretical interest generated by the independence of the frequencies associated with the driving source and the switches, and the natural frequencies of the network.

References for Chapter 2

1. Sun, Y., "Networks Containing Periodic Switches: A Unified Approach and Applications," Ph.D. Thesis, Dept. of Electrical Engineering and Computer Sciences, Univ. of California, Berkeley, September 1967.

2. Liou, M. L. and Mastromonaco, F. R., "Exact Analysis of Linear Circuits Containing a Periodically Operated Switch Using the State Space Approach," IEEE International Symposium on Circuit Theory, Miami Beach, Florida, December 1968.

3. Bryant, P. R., "The Explicit Form of Bashkow's A-Matrix," IRE Trans. on Circuit Theory, Vol. CT-9, pp. 303-306, September 1962.

4. Stern, T. E., Theory of Nonlinear Networks and Systems, Addison-Wesley, Reading, Mass., 1965: Section 2-7.

5. Bedford, B. D. and Hoft, R. G., Principles of Inverter Circuits; New York: John Wiley and Sons, 1964. Chapter 5, pp. 128-149.

CHAPTER 3: SYSTEM FUNCTIONS: DEFINITION AND PROPERTIES

Our main objective in this chapter is the development of a mathematical characterization of SLC networks using time-varying system functions. This development is carried out in Section 3.1. Then in Section 3.2, several relations are derived for the time-varying system functions of one-port and two-port SLC networks based on the lossless condition. This derivation is carried out mostly without specific limitation to SLC networks, so that the results are expected to be valid for other classes of periodically time-varying lossless networks.

Several simple SLC networks are used to illustrate the specialized form of the 2-port relations.

3.1 System Functions

In this section, we further examine the solution represented in equations (9) and (10) of Chapter 2 in order to define, for SLC networks, time-varying system functions of the type introduced by Zadeh. Thereby, we may observe certain properties of these system functions that are identical with those of networks with continuously time-varying elements.

To begin, we may note the fact that in several respects the matrix Q of (2.8c) or (2.19) plays an essential role in the theory of switched networks similar to that of the A-matrix for time-invariant networks. Q is the transition matrix for the discrete system associated with the system (1); i e., if

$$\begin{aligned} \mathring{x} &= A_1 x \ , \ t \in I_{1k} \\ \mathring{x} &= A_2 x \ , \ t \in I_{2k} \end{aligned} \tag{1}$$

then

$$x(kT) = Q^k x_0 \ , \ Q = e^{A_2 T_2} e^{A_1 T_1} \tag{2}$$

and

$$x(t) = \begin{cases} e^{A_1(t-kT)} x(kT) = e^{A_1(t-kT)} Q^k x_0, \ t \in I_{1k} \\ e^{A_2(t-kT-T_1)} x(kT+T_1) = e^{A_2(t-kT-T_1)} e^{A_1 T_1} Q^k x_0, \ t \in I_{2k} \end{cases} \tag{3}$$

The eigenvalues of Q thus determine the transient behavior of the switched network. For SLC networks, which from physical observation are not asymptotically stable, the eigenvalues of Q must all possess unit magnitude such that Q^I is an oscillatory matrix function of the discrete variable k. For example, in the simple circuit shown in Fig. 3-1(a), with $x = \begin{bmatrix} V \\ i \end{bmatrix}$, and

$$A_1 = A_2 = \begin{bmatrix} 0 & -1/C \\ 1/L & 0 \end{bmatrix} = A \; , \tag{4}$$

we find that

$$Q = e^{AT} = \begin{bmatrix} \text{Cos } \omega T & -1/\omega C \text{ Sin } \omega T \\ \frac{1}{\omega L} \text{ Sin } \omega T & \text{Cos } \omega T \end{bmatrix} \tag{5}$$

where $\omega^2 = 1/LC$.

The eigenvalues of Q in (5) are

$$\lambda_{1,2} = \text{Cos } \omega T \pm j \text{ Sin } \omega T \tag{6}$$

so that $|\lambda_1| = 1$ as expected.

For the 2nth-order case, Fig. 3-1(b), where $A_1 = A_2$, Q is the direct sum of 2 x 2 submatrices D_i of the form

$$D_i \begin{bmatrix} \text{Cos } \omega_i T & -\frac{1}{\omega_i C_i} \text{ Sin } \omega_i T \\ \frac{1}{\omega_i L_i} \text{ Sin } \omega_i T & \text{Cos } \omega_i T \end{bmatrix} \tag{7}$$

where $\omega_i{}^2 = \frac{1}{L_i C_i}$.

Thus, in this case, even when some eigenvalues of Q coincide, while each has unit magnitude, Q does not have any unbounded growing modes. We note that two eigenvalues of Q are equal whenever

$$\omega_i = \omega_j \pm \frac{2\pi k}{T} \tag{8}$$

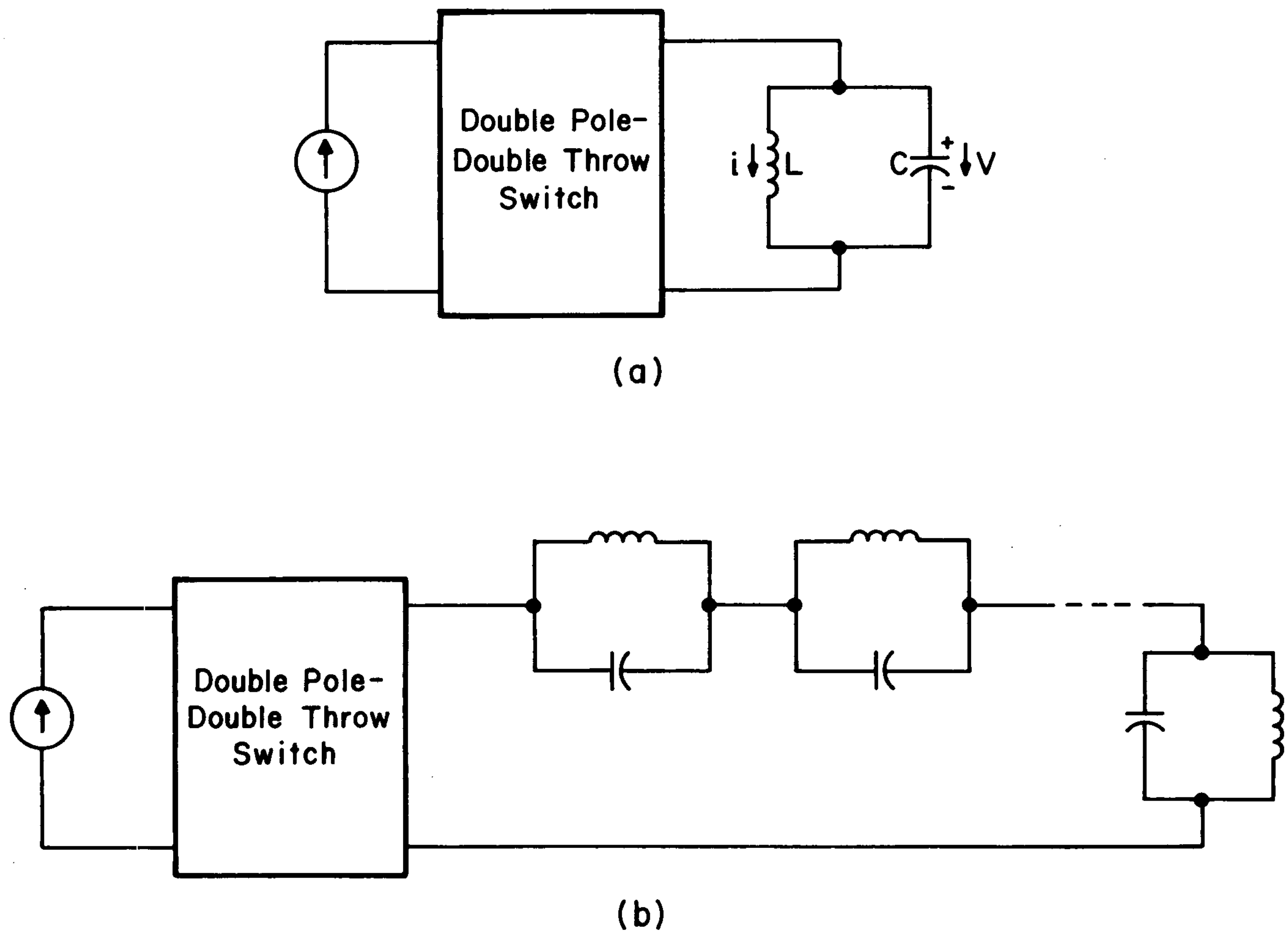

FIG. 3.1 EXAMPLES OF SLC NETWORKS

for some (i,j). For the case $A_1 \neq A_2$, but with the same ordering of state-variables, the eigenvalues of Q are of the form

$$\lambda_{g_i} = \text{Cos } \alpha_{g_i} \pm j \text{ Sin } \alpha_{g_i} \tag{9}$$

where $\alpha_{g_i} = \omega_{1i}\delta T + \omega_{2i}(1-\delta)T$

$\delta = T_1/T$ = duty cycle

ω_{j_i} = i^{th} natural frequency of network in time interval I_{jk} = i^{th} eigenvalue of matrix A_j.

As the behavior of Q^k for SLC networks is closely related to that of e^{AT} for LC networks, so a steady-state response for SLC networks may be defined in a manner analogous to that of LC networks. For LC networks described by the equation

$$\mathring{x} = Ax + Be^{pt} \tag{10}$$

the complete solution is

$$x(t) = e^{At}x_0 - e^{At}(pI-A)^{-1}B + (pI-A)^{-1}B\ e^{pt}. \tag{11}$$

Here e^{At} is oscillatory and the limit of e^{At} as $t\to\infty$ does not exist. Then we may not define a steady-state solution simply by a time translation approaching infinity. But a "steady-state" solution may be defined by choosing the particular set of initial conditions

$$x_0 = (pI-A)^{-1}B \tag{12}$$

so that the oscillatory transient represented by the first two terms in (11) is not launched. Then

$$x_{s_s}(t) = (pI-A)^{-1}B\ e^{pt}\ . \tag{13}$$

For SLC networks, we may similarly choose the particular set of initial conditions

$$Z_0 = (I-Q)^{-1}G \tag{14}$$

for equation (9) and thus obtain

$$Z_{s_s}(kT) = Z_1 = (I-Q)^{-1}G \tag{15a}$$

$$Z_{s_s}(kT+T_1) = Z_2 = Q_1(I-Q)^{-1}G + G_1 \tag{15b}$$

Then the steady-state solution may be written as

$$x(t) = N(p,t)\ e^{pt} \tag{16}$$

where

$$N(p,t) = \begin{cases} e^{E_1(t-kT)}\left[Z_1 + E_1^{-1}B_1\right], & t \in I_{2k} \\ e^{E_2(t-kT-T_1)}\left[Z_2 + E_2^{-1}B_2\right] - E_2^{-1}B_2, & t \in I_{2k} \end{cases} \tag{17}$$

The resulting $N(p,t)$ is a vector-valued, time-varying system function of the type defined by Zadeh.[1] The poles of $N(p,t)$, arising from the term $(I-Q)^{-1}G$ in Z_1 and Z_2, are time-invariant, in agreement with the result proved by Darlington[2] for networks all of whose elements vary periodically with the same period. The poles contributed by the factor G are the natural frequencies of the network in both time intervals, as observed in the inverse operations implicit in the expression

$$G = Q_2(I-Q_1)(pI-A_1)^{-1}B_1 + (I-Q_2)(pI-A_2)^{-1}B_2 \tag{8}$$

By a procedure similar to that employed earlier in the discussion of the eigenvalues of Q, the poles resulting from the factor

$(I-Q)^{-1}$ can be shown to be of the form

$$P_{k_i} = j(\omega_i + k\omega_s) \ , \ i = 1,2, \cdots M \qquad k = 0, \pm 1, \pm 2,.. \tag{19}$$

where $\omega_s = \frac{2\pi}{T}$ is the switching frequency.

For the special case when A_1 and A_2 have the same eigenvalues, the quantities ω_i in (19) are the natural frequencies of the network. In general,

$$\omega_i = \omega_{i_1}\delta + \omega_{i_2}(1-\delta) \tag{20}$$

where the frequencies are defined in a manner similar to the definition of the eigenvalues in equation (9).

Since the poles of the system function $N(p,t)$ all lie on the imaginary axis, SLC networks have an infinite number of real resonant frequencies, any one of which could produce driven instability. For example, the "ringing choke" circuit shown in Fig. 3-2 is known to have an unbounded mode when the input voltage is d.c. and the switching frequency, ω_s, equals the natural frequency in I_{2k}, $\omega_2 = 1/\sqrt{LC}$. In this case, the driving frequency zero is just one of the infinite resonant frequencies

$$\omega_k = \omega_s(1+k) \ , \ k = 0, \pm 1,...$$

for which the circuit possesses an unbounded mode due to resonance.

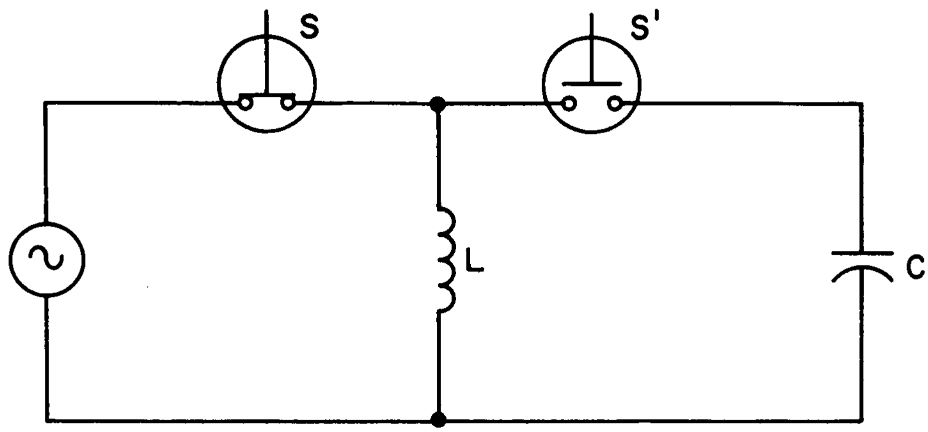

FIG. 3.2 "RINGING-CHOKE" CIRCUIT

Considering next the time domain aspects of $N(p,t)$, we observe directly that $N(p,t)$ is periodic in t with period T, the common switching period, also in agreement with the known results for periodically varying networks. Fourier expansion of $N(p,t)$ then defines the bandlimited system functions $N_k(p)$, which have the following property: If the system with response function $N(p,t)$ is followed in cascade by an ideal bandpass filter of bandwidth ω_s centered at frequency $k\omega_s$ as in Fig. 3-3, the response function of the total system is then $N_k(p)e^{jk\omega_s t}$.

From equation (17) we obtain by direct integration,

$$N(p,t) = \sum_{k=-\infty}^{\infty} N_k(p)e^{jk\omega_s t} \ , \ \omega_s = \frac{2\pi}{T} \ , \tag{21}$$

where

$$\begin{aligned} N_k(p) = \frac{1}{T} \Big\{ & \left[(p + jk\omega_s)I-A_1\right]^{-1}\left[I-e^{[A_1-(p+jk\omega_s)I]T_1}\right]\left[Z_1+E_1^{-1}B_1\right] \\ & + e^{-jk\omega_s T_1}\left[(p + jk\omega_s)I-A_2\right]^{-1}\left[I-e^{[A_2-(p+jk\omega_s)I]T_2}\right]\left[Z_2+E_2^{-1}B_2\right] \\ & + \left[(pI-A_1)^{-1}B_1 - (pI-A_2)^{-1}B_2\right]\left[\frac{1-e^{-jk\omega_s T_1}}{jk}\right]\Big\} \end{aligned} \tag{22}$$

The most commonly encountered of the bandlimited system functions is $N_0(p)$, for which the bandlimiting filter is an ideal lowpass filter. Setting $k\to 0$ in equation (22) gives

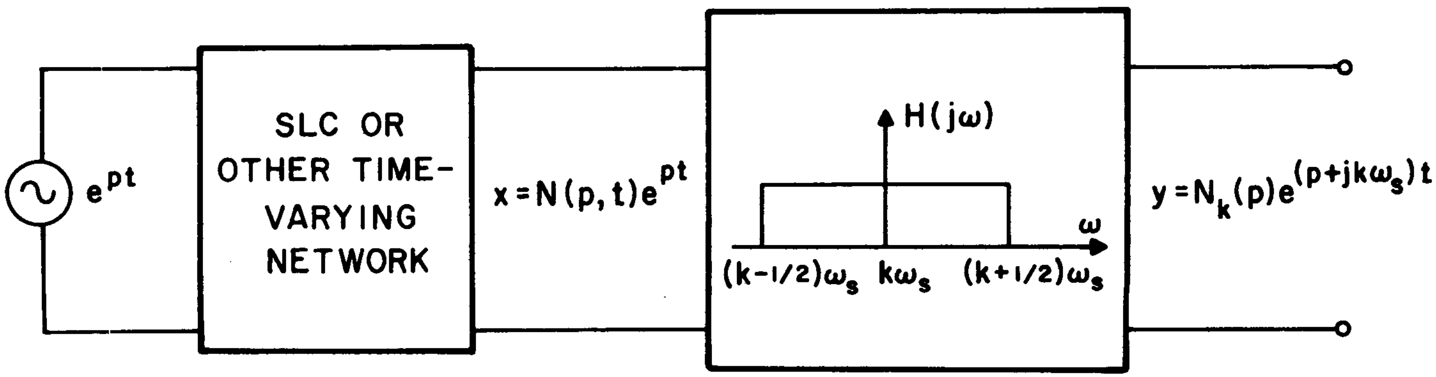

FIG. 3.3 BANDLIMITED SYSTEM FUNCTIONS

$$N_0(p) = \frac{1}{T}\Big\{(pI-A_1)^{-1}(I-Q_1)(Z_1+E_1{}^{-1}B_1)$$

$$+ (pI-A_2)^{-1}(I-Q_2)(Z_2+E_2{}^{-1}B_2) \qquad (23)$$

$$+ T_1[(pI-A_1)^{-1}B_1 - (pI-A_2)^{-1}B_2]\Big\}$$

As an example, consider the switched capacitor circuit shown in Fig. 3-4(a).

Here $\quad A_1 = A_2 = B_2 = 0 \,,\; B_1 = 1$

Then $\quad Q_1 = e^{-pT_1} \,,\; Q_2 = e^{-pT_2} \,,\; Q = e^{-pT}$

$$G_1 = \frac{1-e^{-pT_1}}{p} \,,\; G_2 = 0$$

$$G = \frac{e^{-pT_2}-e^{-pT}}{p}$$

$$Z_1 = \frac{e^{-pT_2}-e^{-pT}}{p(1-e^{-pT})}$$

$$Z_2 = \frac{1-e^{-pT_1}}{p(1-e^{-pT})}$$

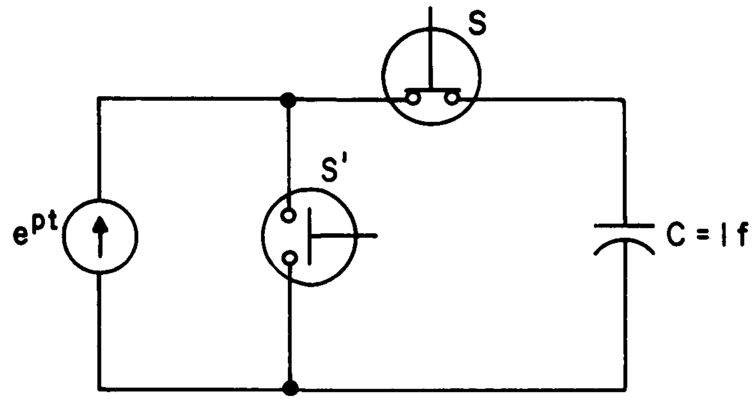

(a) SINGLE SWITCHED CAPACITOR

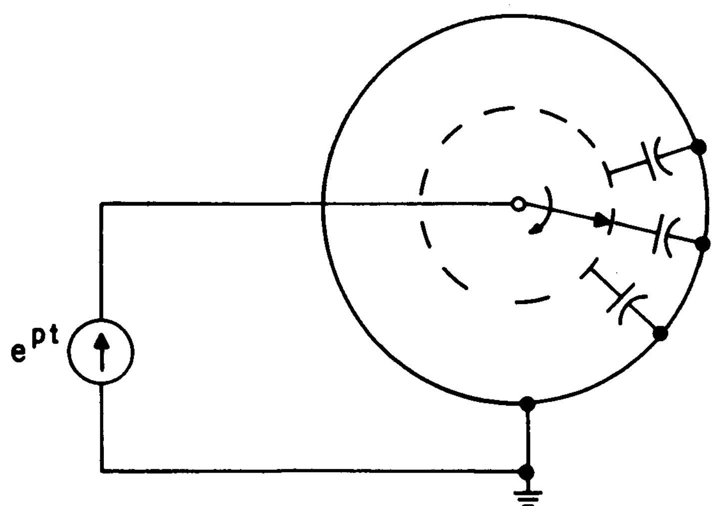

(b) COMMUTATED N-CAPACITOR NETWORK

FIG. 3.4 SWITCHED-CAPACITOR NETWORKS

Hence

$$N_k(p) = \frac{1}{T}\left\{\frac{\left[1-e^{-(p+jk\omega_s)T_1}\right]\left[e^{-pT_2}-1\right]+e^{-jk\omega_sT_1}\left[1-e^{-pT_1}\right]\left[1-e^{-(p+jk\omega_s)T_2}\right]}{p(p+jk\omega_s)(1-e^{-pT})} + \frac{1}{p}\left(\frac{1-e^{-jk\omega_sT_1}}{jk}\right)\right\} .$$

In particular, $N_0(p)$ is simply given by

$N_0(p) = \left(\frac{T_1}{T}\right)\frac{1}{p}$, the only effect of the switching being to multiply the capacitance by the ratio $\frac{T}{T_1}$.[3]

For the n-capacitor uniformly commutated network shown in Fig. 3-4(b), however, the transfer function possesses an additional multiplicative factor

$$\sum_{k=0}^{n} e^{-k(pT/n)} = \frac{1-e^{-pT}}{1-e^{-pT/n}}$$

due to the uniform delays in observing the response of individual capacitors at the overall circuit output. The singularities of this extra factor produce both comb-like and band-pass characteristics so that the circuit has been utilized in various configurations for radar signal processing applications and inductorless bandpass filter realization.[4,5]

3.2: Further Properties of System Functions: Consequences of Lossless Condition

In this section, we shall explore further properties of system functions of 1-port and 2-port SLC networks which are consequences of the lossless condition. These properties are found to be generalizations of familiar cases for LC networks.

First, consider the dual 1-port SLC networks shown in Fig. 3-5. For Fig. 3-5(a), if the input is

$$i(t) = \mathrm{Re}\left\{e^{j\omega t}\right\} = \mathrm{Cos}\ \omega\ t$$

then the voltage across the terminals of the network at port 1 is

$$v(t) = \mathrm{Re}\left\{Z(j\omega,t)e^{j\omega t}\right\} \tag{24}$$

by the principle of superposition for linear systems. Let $Z(j\omega,t)$ be separated into real and imaginary parts as

$$Z(j\omega,t) = R(\omega,t) + jX(\omega,t) \quad . \tag{25}$$

Then $$v(t) = R(\omega,t)\ \mathrm{Cos}\ \omega t - X(\omega,t)\ \mathrm{Sin}\ \omega t$$

and the instantaneous power absorbed by the network at port 1 is

$$p(t) = v(t)i(t) = R(\omega,t)\ \mathrm{Cos}^2\omega t - X(\omega,t)\ \mathrm{Sin}\ \omega t\ \mathrm{Cos}\ \omega t$$

$$= \frac{1}{2}\left\{R(\omega,t)[1 + \mathrm{Cos}\ 2\ \omega t] - X(\omega,t)\ \mathrm{Sin}\ 2\ \omega t\right\} .$$

Since the network is lossless, the time average of the power absorbed is zero, i.e.,

$$\langle p(t)\rangle = \frac{1}{2}\left\{\langle R(\omega,t)\rangle + \langle R(\omega,t)\ \mathrm{Cos}\ 2\ \omega t\rangle - \langle X(\omega,t)\ \mathrm{Sin}\ 2\ \omega t\rangle\right\} = 0. \tag{26}$$

Since $Z(j\omega,t)$ is periodic in time with period $T = 2\pi/\omega_s$, so also are $R(\omega,t)$ and $X(\omega,t)$. Thus, for $\omega_s \neq 2\omega$,

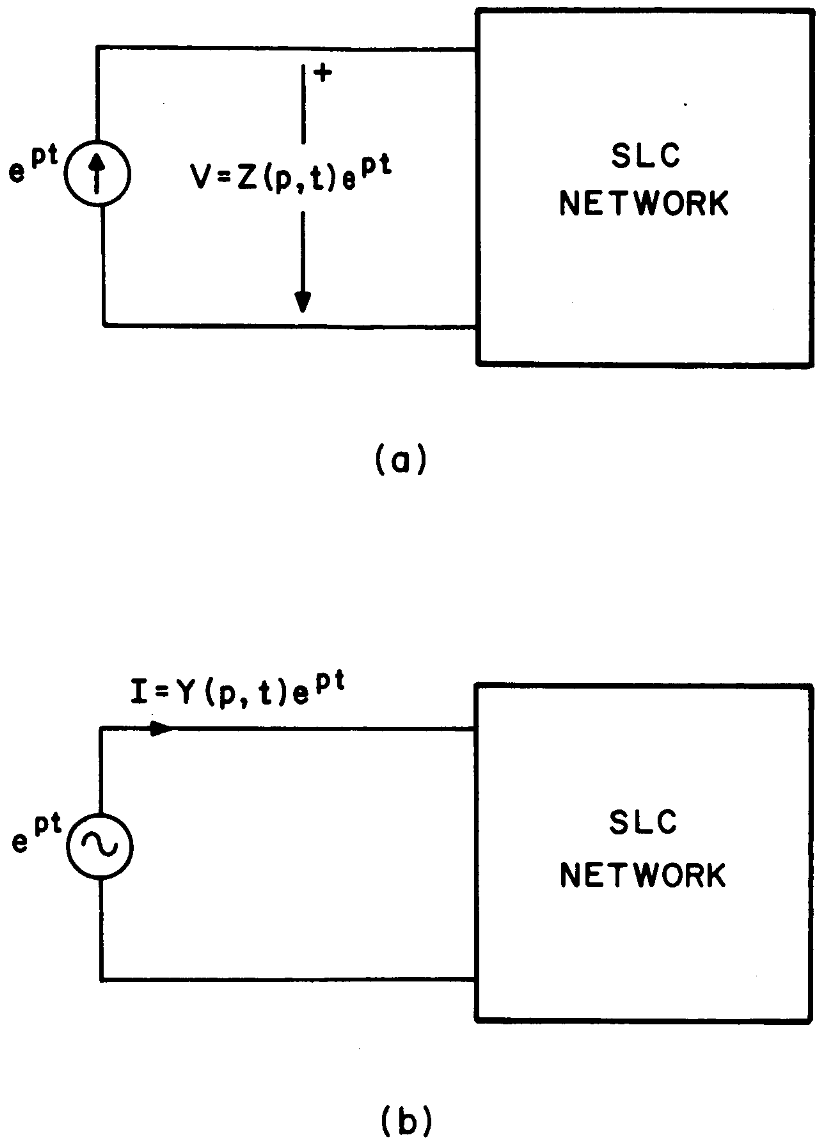

FIG. 3.5 SLC 1-PORT NETWORKS

$$\langle R(\omega,t) \text{ Cos } 2\ \omega t \rangle = \langle X(\omega,t) \text{ Sin } 2\ \omega t \rangle = 0 \ .$$

For $\omega_s = 2\omega$, let

$$Z(j\omega,t) = \sum_{k=-\infty}^{\infty} Z_k(j\omega) e^{jk\omega_s t} \tag{27}$$

where we may write

$$Z_k(j\omega) = R_k(\omega) + jX_k(\omega) \tag{28}$$

Then

$$R(\omega,t) = \sum_{k=-\infty}^{\infty} \left[R_k(\omega) \text{ Cos } k\ \omega_s t - X_k(\omega) \text{ Sin } k\ \omega_s t\right]$$

$$X(\omega,t) = \sum_{k=-\infty}^{\infty} \left[R_k(\omega) \text{ Sin } k\ \omega_s t + X_k(\omega) \text{ Cos } k\ \omega_s t\right] \ .$$

Hence

$$\langle R(\omega,t) \text{ Cos } 2\ \omega t \rangle = \frac{1}{2} R_2(\omega)$$

$$\langle X(\omega,t) \text{ Cos } 2\ \omega t \rangle = \frac{1}{2} R_2(\omega)$$

so that

$$\langle R(\omega,t) \text{ Cos } 2\ \omega t \rangle - \langle X(\omega,t) \text{ Sin } 2\ \omega t \rangle = 0 \ .$$

Hence

$$\langle p(t) \rangle = \langle R(\omega,t) \rangle = 0$$

or from the periodicity and definition of $R(\omega,t)$ we obtain

$$\int_0^T \text{Re}\left\{Z(j\omega,t)\right\} dt = 0 \tag{29a}$$

for all ω, $\omega_s = 2\pi/T$. This is then the generalization, for the time-varying case, of the relation

$$\text{Re}\left\{Z_{LC}(j\omega)\right\} = 0$$

for time-invariant reactance functions.

By a similar procedure starting with Fig. 3-5(b), we also have

$$\langle \mathrm{Re}\left\{Y(j\omega,t)\right\}\rangle = 0 \tag{29b}$$

We next consider the SLC 2-port network terminated at port 2 by a passive time-invariant impedance, Fig. 3-6.
Let the driving voltage be

$$v(t) = \mathrm{Re}\left\{e^{j\omega t}\right\} = \mathrm{Cos}\ \omega t\ .$$

Then

$$i_1(t) = \mathrm{Re}\left\{Y_{11}(j\omega,t)e^{j\omega t}\right\}$$

$$= G_{11}(\omega,t)\ \mathrm{Cos}\ \omega t - B_{11}(\omega,t)\ \mathrm{Sin}\ \omega t$$

and

$$\begin{aligned} i_2(t) &= \mathrm{Re}\left\{Y_{21}(j\omega,t)e^{j\omega t}\right\} \\ &= G_{21}(\omega,t)\ \mathrm{Cos}\ \omega t - B_{21}(\omega,t)\ \mathrm{Sin}\ \omega t \end{aligned} \tag{30}$$

where

$$Y_{11}(j\omega,t) = G_{11}(\omega,t) + jB_{11}(\omega,t) \tag{31}$$

$$Y_{21}(j\omega,t) = G_{21}(\omega,t) + jB_{21}(\omega,t) \tag{32}$$

are the driving point and transfer admittance functions, respectively, of the loaded 2-port at ports 1 and 2.

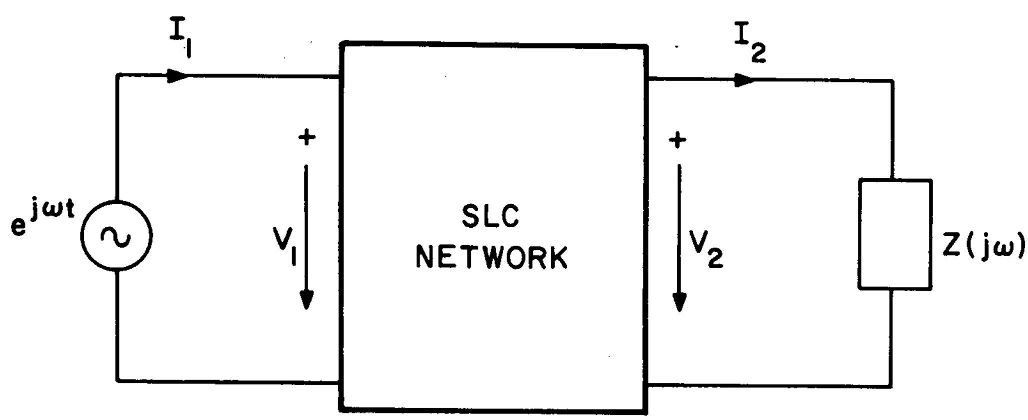

FIG. 3.6 SLC NETWORK TERMINATED WITH PASSIVE IMPEDANCE

Since, from the results of the previous section, $Y_{21}(j\omega,t)$ is periodic in time with period $T = \frac{2\pi}{\omega_s}$, it may be expanded in the Fourier Series

$$Y_{21}(j\omega,t) = \sum_{k=-\infty}^{\infty} Y_{21_k}(j\omega)e^{jk\omega_s t} \tag{33}$$

For every component, $I_n e^{j\omega_n t}$, of the current I_2, there corresponds a component for the voltage V_2 of value $Z(j\omega_n)I_n e^{j\omega_n t}$ on account of the linearity and time invariance of the impedance $Z(j\omega)$. Hence by superposition, for the current $i_2(t)$ given by equation (30), we have the voltage across the impedance

$$V_2(t) = \text{Re}\left\{\sum_{k=-\infty}^{\infty} Z(j\omega_k)Y_{21_k}(j\omega)e^{j\omega_k t}\right\} \tag{34}$$

where

$$\omega_k = \omega + k\omega_s \ .$$

Let

$$Z(j\omega) = R(\omega) + jX(\omega) \tag{35}$$

$$Y_{21_k}(j\omega) = G_{21_k}(\omega) + jB_{21_k}(\omega) \tag{36}$$

and define

$$R_k = R(\omega_k)$$

$$X_k = X(\omega_k) \ .$$

Then

$$v_2(t) = \sum_{k=-\infty}^{\infty} R_k \left[G_{21_k} \text{ Cos } \omega_k t - B_{21_k} \text{ Sin } \omega_k t \right]$$

$$-X_k \left[G_{21_k} \text{ Sin } \omega_k t + B_{21_k} \text{ Cos } \omega_k t \right]$$

$$= \sum_{k=-\infty}^{\infty} \left(R_k G_{21_k} - X_k B_{21_k} \right) \text{ Cos } \omega_k t$$

$$- \left(R_k B_{21_k} + X_k G_{21_k} \right) \text{ Sin } \omega_k t \tag{37}$$

Also from equations (30), (33) and (36), we have

$$i_2(t) = \sum_{k=-\infty}^{\infty} G_{21_k} \text{ Cos } \omega_k t - B_{21_k} \text{ Sin } \omega_k t \tag{38}$$

As for the 1-port considered earlier, the instantaneous power absorbed at port 1 is

$$p_1(t) = v_1(t)\ i_1(t)$$

$$= G_{11}(\omega,t) \text{ Cos}^2\ \omega t - B_{11}(\omega,t) \text{ Sin } \omega t \text{ Cos } \omega t$$

and the average power is

$$\langle p_1(t) \rangle = \frac{1}{2} \langle G_{11}(\omega,t) \rangle = \frac{1}{2T} \int_0^T \text{Re}\left\{ Y(j\omega,t) \right\} dt \tag{39}$$

The power dissipated by the passive impedance is

$$p_2(t) = v_2(t)\, i_2(t)$$

$$\begin{aligned} = \sum_m \sum_n \Big\{ & G_{21_m}\left(R_n G_{21_n} - X_n B_{21_n}\right) \text{Cos } \omega_m t \text{ Cos } \omega_n t \\ & - G_{21_m}\left(R_n B_{21_n} + X_n G_{21_n}\right) \text{Cos } \omega_m t \text{ Sin } \omega_n t \\ & - B_{21_m}\left(R_n G_{21_n} - X_n B_{21_n}\right) \text{Sin } \omega_m t \text{ Cos } \omega_n t \\ & + B_{21_m}\left(R_n B_{21_n} + X_n G_{21_n}\right) \text{Sin } \omega_m t \text{ Sin } \omega_n t \Big\} \end{aligned} \tag{40}$$

Hence

$$\begin{aligned} \langle p_2(t) \rangle = \frac{1}{2} \sum_k & G_{21_k}\left(R_k G_{21_k} - X_k B_{21_k}\right) \\ & + G_{21_k}\left(R_k B_{21_k} + X_k G_{21_k}\right) \end{aligned} \tag{41}$$

i.e.,

$$\langle p_2(t) \rangle = \frac{1}{2} \sum_{k=-\infty}^{\infty} R_k\left(G^2_{21_k} + B^2_{21_k}\right)$$

Finally, from the losslessness of the coupling SLC network, we equate $\langle p_1(t) \rangle = \langle p_2(t) \rangle$ and obtain

$$\langle G_{11}(\omega,t) \rangle = \sum_{k=-\infty}^{\infty} R(\omega_k) \left|Y_{21_k}(j\omega)\right|^2 \tag{42}$$

We note two special cases of equation (42). First, if the terminating passive impedance is a pure resistance R independent of frequency, the right-hand-side of the equation reduces to

$$R \sum_{k=-\infty}^{\infty} |Y_{21_k}(j\omega)|^2$$

and since $Y_{21}(j\omega,t)$ is at least piecewise continuous as a function of t,

$$\sum_{k=-\infty}^{\infty} |Y_{21_k}(j\omega)|^2 = \frac{1}{T}\int_0^T |Y_{21}(j\omega,t)|^2 \, dt$$

by Parseval's theorem.

Hence, finally, we have

$$\langle \mathrm{Re}\{Y_{11}(j\omega,t)\}\rangle = R\langle |Y_{21}(j\omega,t)|^2 \rangle \tag{43}$$

which for $R = 1\Omega$ is seen as a generalization of the relation,

$$\mathrm{Re}\{Y_{11}(j\omega)\} = |Y_{21}(j\omega)|^2$$

or its dual form

$$\mathrm{Re}\{Z_{11}(j\omega)\} = |Z_{21}(j\omega)|^2$$

which are used in the Darlington synthesis of passive time-invariant impedances by lossless networks terminated by a unit resistance.

Another special case is that where the passive impedance $Z(j\omega)$ is a reactance function. Then $R(\omega) \equiv 0$ and equation (42) reduces simply to equation (29) since now the whole system is a SLC network as seen from port 1.

We may also note the dual form of equation (42):

$$\langle \text{Re } Z_{11}(j\omega,t) \rangle = \sum_{k=-\infty}^{\infty} G(\omega_k) \left| Z_{21_k}(j\omega) \right|^2 \tag{44}$$

Finally, by a similar procedure on the doubly terminated network of Fig. 3-7 , we obtain the relation

$$\langle \text{Re}\{Y_{11}(j\omega,t)\} \rangle = \sum_{k=-\infty}^{\infty} R_1(\omega_k) \left| Y_{11_k}(j\omega) \right|^2 + R_2(\omega_k) \left| Y_{21_k}(j\omega) \right|^2 \tag{45}$$

where the system functions are defined by the equations

$$Z_1(j\omega) = R_1(\omega) + j\, X_1(\omega)$$

$$Z_2(j\omega) = R_2(\omega) + j\, X_2(\omega)$$

$$I_1 = Y_{11}(j\omega,t)e^{j\omega t}$$

$$I_2 = Y_{21}(j\omega,t)e^{j\omega t}$$

$$V_1 = e^{j\omega t} - \sum_k Z_1(j\omega_k)Y_{11_k}(j\omega)e^{j\omega_k t}$$

$$V_2 = \sum_k Z_2(j\omega_k)Y_{21_k}(j\omega)e^{j\omega_k t}$$

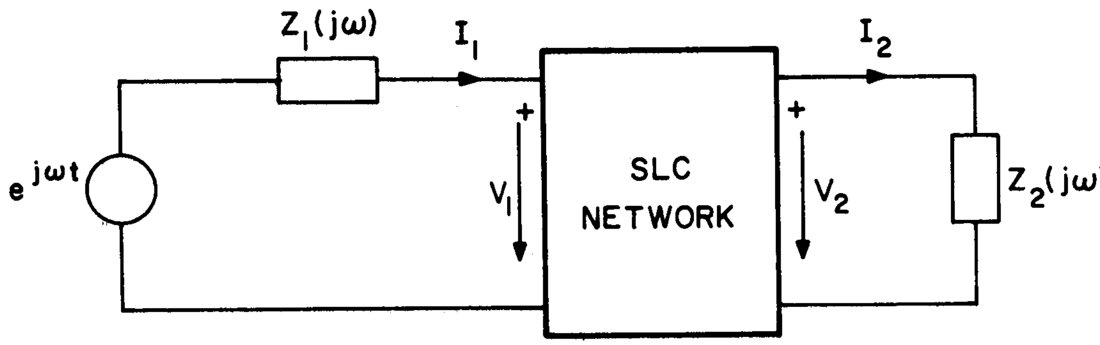

FIG. 3.7 DOUBLY-TERMINATED SLC 2-PORT

The relations derived in this section are of theoretical interest as extensions of classical frequency domain properties of LC network functions. Since the system functions are not rational in the variable p, the relations between driving point and transfer immittances do not lead to a complete or partial specification of either class of functions. Still, the results are expected to be of further use in a complete treatment of the synthesis of linear time-varying networks.

3.3 Examples

In the previous section, we derived several relations among system functions of linear, lossless time-varying networks under passive time-invariant loads. The derivation was quite general and the results are not limited to SLC networks alone but apply to any lossless time-varying network for which the appropriate system functions are defined. In this section, we shall utilize several first order SLC networks to illustrate the validity of the results.

Example 1. For the circuit shown in Fig. 3-7(a),

$$I_1 = I_2 = \begin{cases} \frac{1}{R}\, e^{j\omega t} & , \quad t \in I_{1k} \quad \text{(switch closed)} \\ 0 & , \quad t \in I_{2k} \quad \text{(switch open)} \end{cases}$$

From the defining relations

$$I_1 = Y_{11}(j\omega,t)e^{j\omega t} ,$$

$$I_2 = Y_{21}(j\omega,t)e^{j\omega t} ,$$

we obtain

$$Y_{11}(j\omega,t) = Y_{21}(j\omega,t) = \begin{cases} \frac{1}{R} & , \quad t \in I_{1k} \\ 0 & , \quad t \in I_{2k} \end{cases}$$

We can thus verify directly that

$$\langle \mathrm{Re}\{Y_{11}(j\omega,t)\}\rangle = \frac{1}{2R} = R\ \langle |Y_{21}(j\omega,t)|^2 \rangle$$

in accordance with equation (43).

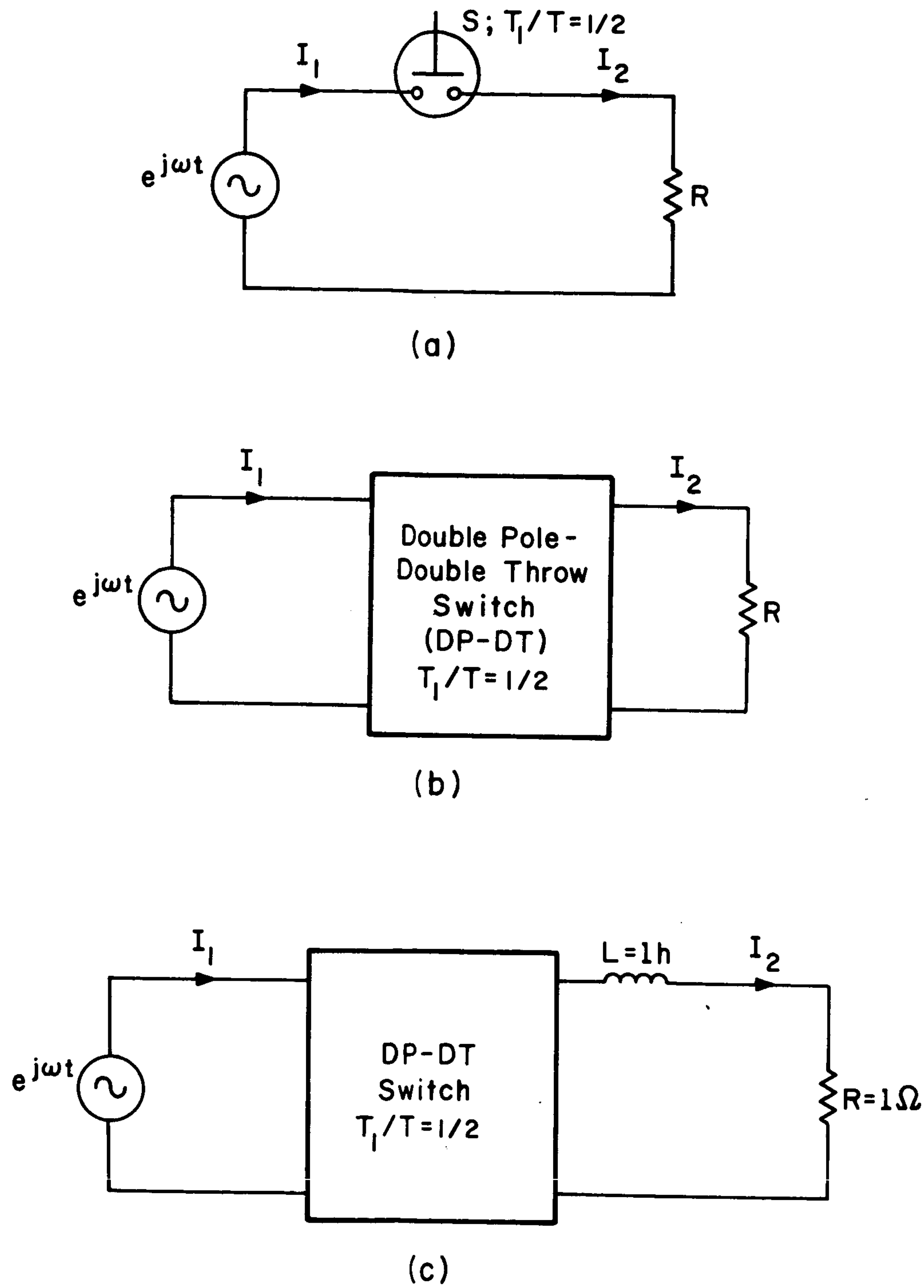

FIG. 3.8 EXAMPLES

Example 2:

For the circuit shown in Fig. 3-7(b), we have

$$I_2 = \begin{cases} \frac{1}{R} e^{j\omega t} , & t \in I_{1k} \\ -\frac{1}{R} e^{j\omega t} , & t \in I_{2k} \end{cases}$$

and

$$I_1 = \begin{cases} \frac{1}{R} e^{j\omega t} , & t \in I_{1k} \\ \frac{1}{R} e^{j\omega t} , & t \in I_{2k} \end{cases}$$

Hence

$$Y_{11}(j\omega,t) = \frac{1}{R}$$

and $$\langle \mathrm{Re}\{Y_{11}(j\omega,t)\}\rangle = \frac{1}{R} .$$

Also

$$Y_{21}(j\omega,t) = \begin{cases} \frac{1}{R} , & t \in I_{1k} \\ -\frac{1}{R} , & t \in I_{2k} \end{cases}$$

and $$\langle |Y_{21}(j\omega,t)|^2 \rangle = \frac{1}{R^2} .$$

Again the results agree with equation (43).

Example 3:

We next consider the circuit of Fig. 3-7(c). Using the identical symbols of Chapter 2, we have

$$A_1 = A_2 = 1 , B_1 = 1 , B_2 = -1 .$$

Substituting these values in the summary of response equations given in Section 2.4, we obtain expressions for the system functions as follows:

$$Y_{11}(p,t) = \begin{cases} e^{-(p+1)(t-kT)}\left[Z_1-1\right]+1\ , & t\in I_{1k} \\ e^{-(p+1)(t-kT-1/2\ T)}\left[Z_1-1\right]+1\ , & t\in I_{2k} \end{cases}$$

$$Y_{21}(p,t) = \begin{cases} e^{-(p+1)(t-kT)}\left[Z_1-1\right]+1\ , & t\in I_{1k} \\ e^{-(p+1)(t-kT-1/2\ T)}\left[-Z_1+1\right]-1\ , & t\in I_{2k} \end{cases}$$

where $$Z_1 = \frac{-\left(1-e^{-T/2}e^{-pT/2}\right)^2}{\left(p+1\right)\left(1-e^{-T}e^{-pT}\right)} .$$

It is algebraically cumbersome to compute the expressions for the quantities

$$\langle \mathrm{Re}\left\{Y_{11}(j\omega,t)\right\}\rangle \quad \text{and} \quad \langle |Y_{21}(j\omega,t)|^2\rangle$$

for arbitrary values of ω. But we can verify the validity of equation (43) for the particular value, $\omega = 0$.

Setting $p = 0$, we have

$$Y_{11}(0,t) = \begin{cases} 1 + C\ e^{-(t-kT)}\ , & t\in I_{1k} \\ 1 + C\ e^{-(t-kT-1/2\ T)}\ , & t\in I_{2k} \end{cases}$$

and

$$Y_{21}(0,t) = \begin{cases} 1 + C\ e^{-(t-kT)} & , t \in I_{1k} \\ -1 - C\ e^{-(t-kT-1/2\ T)} & , t \in I_{2k} \end{cases}$$

where

$$C = \frac{-2\left(1-e^{-T/2}\right)}{1-e^{-T}} .$$

By direct integration, we have

$$\langle \mathrm{Re}\left\{Y_{11}(0,t)\right\}\rangle = \frac{1}{T}\left[T+2C(1-e^{-T/2})\right]$$

$$\langle |Y_{21}(0,t)|^2 \rangle = \frac{1}{T}\left[T+4C(1-e^{-T/2}) + C^2(1-e^{-T})\right] .$$

Substituting the value of C, we verify directly that these two expressions are identical.

References for Chapter 3

1. Zadeh, L. A., "Frequency Analysis of Variable Networks," Proc. IRE, Vol. 38, March 1950, pp. 291-299.
2. Darlington, S., "An Introduction to Time-Variable Networks," Proc. of the Midwest Symposium on Circuit Analysis, Univ. of Illinois, 1955, pp. 5-1 to 5-25.
3. Sun, Y. and Frisch, I. T., "Resistance Multiplication in Integrated Circuits by Means of Switching," IEEE Trans. on Circuit Theory, Vol. CT-15, pp. 184-192, Sept. 1968.
4. LePage, W. R., Cahn, C. R. and Brown, J. S., "Analysis of a Comb Filter Using Synchronously Commutated Capacitors," AIEE Trans., Part 1, Vol. 72, pp. 63-68, March 1953.
5. Smith, B. D., "Analysis of Commutated Networks," IRE Trans., PGAE-10, pp. 21-26, Dec. 1953.

Chapter 4: FREQUENCY-POWER RELATIONS AND PRACTICAL CONSIDERATIONS

Frequency-power formulas[1] are consequences of the principle of conservation of energy and the fact that two or more frequencies can be specified independently for a system. In the context of this thesis, we have frequency ω associated with the signal or power source and frequency ω_s associated with the switch. Since the pioneering work of Manley and Rowe[2] on nonlinear reactors with two independent frequencies, frequency-power equations and inequalities have been derived by several authors for many systems, both electrical and nonelectrical. In general treatments,[3-5] the formulas involve an arbitrary but finite number of independent frequencies while the generated frequencies, for general forms of nonlinearities, are regarded as arbitrary functions of the input frequencies. More specialized forms have also been given for simple frequency structures and particular forms of nonlinearities.[6-8] These formulas have been useful in obtaining some fundamental bounds on the maximum theoretical efficiency that can be achieved in frequency-conversion systems. Since the ideal switch is a degenerate nonenergic element with no single-valued V-I function defined, earlier methods of deriving frequency-power formulas which involve energy functions are not directly applicable. However, with the form of the solution and properties of the system functions derived in Chapters 2 and 3 at hand, we may, following the technique used by later authors[9,10] obtain useful frequency-power relations by direct computation of the power associated with the voltage and current components at various frequencies supplied externally or generated internally by the network.

In Sections 4.1 and 4.2, several frequency power relations are derived for the class of SLC networks. Also in Section 4.2 is a discussion of the lack of strict fundamental constraints such as Page's Law on the conversion efficiency of SLC networks. This is illustrated by a simple circuit for harmonic generation. Section 4.3 deals with further practical aspects of SLC networks in comparison with nonlinear resistive and reactive networks.

4.1 Reactive Power Formulas

Consider the SLC network divided into multiport subnetworks as shown in Fig. 4-1.

For an input function $e^{j\omega t}$, the capacitor voltages are

$$V_c = N_c(j\omega,t)e^{j\omega t} \tag{1}$$

where the vector function $N_c(j\omega,t)$ is periodic in time with period T.

Hence

$$V_c = \sum_{k=-\infty}^{\infty} N_{c_k}(j\omega)e^{j(\omega+k\omega_s)t} \tag{2}$$

where

$\omega_s = 2\pi/T$ is the switching frequency.

Since each capacitive element is linear and time-invariant, the capacitor currents are given by

$$I_c = \sum_{k=-\infty}^{\infty} j(\omega+k\omega_s)C\ N_{c_k}(j\omega)e^{j(\omega+k\omega_s)t} \tag{3}$$

where C = diagonal $[C_i]$ is the matrix of the capacitances.

Equations (2) and (3) simply state that if the component of capacitor voltage at the frequency $\omega + k\omega_s$ is

$$V_{c_k} = N_{c_k}(j\omega)e^{j(\omega+k\omega_s)t}$$

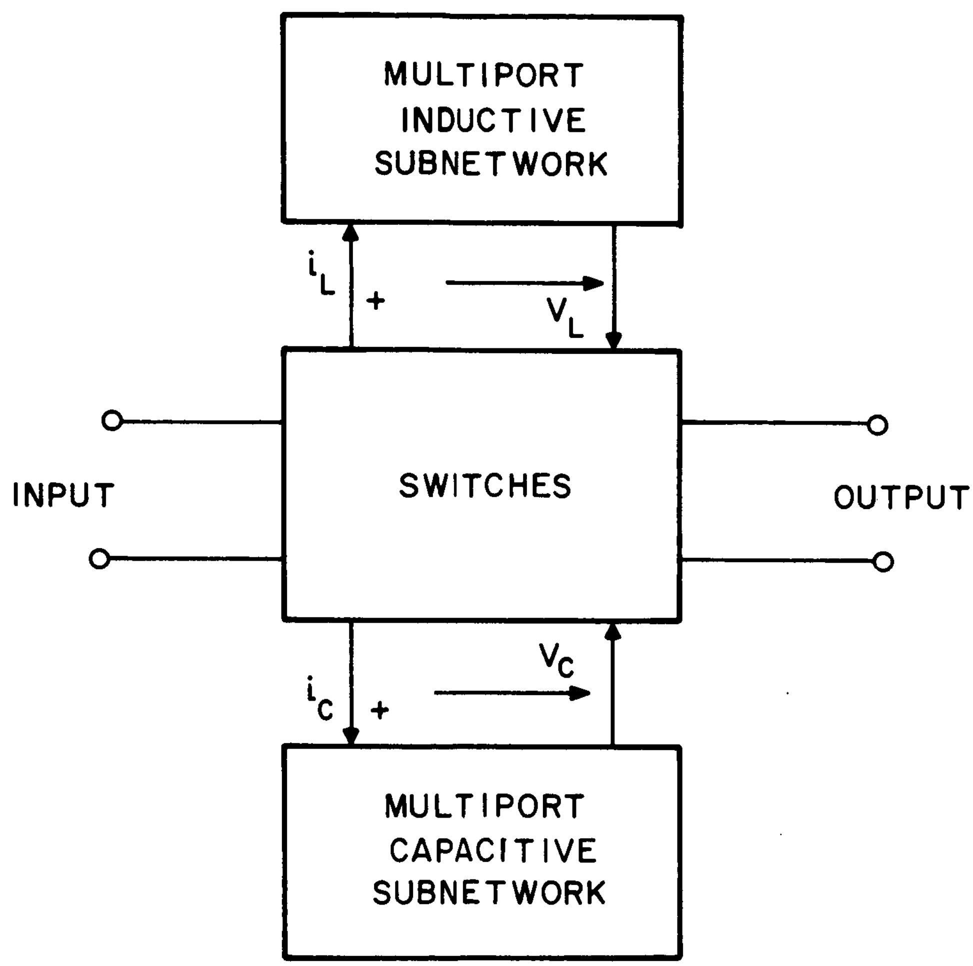

FIG. 4.1 MULTIPORT SUBNETWORKS OF SLC NETWORK

then the component of capacitor current at that frequency is

$$I_{c_k} = j(\omega+k\omega_s)C\, N_{c_k}(j\omega)e^{j(\omega+k\omega_s)t} \quad .$$

The simple form of the relation between V_{c_k} and I_{c_k} is not possible for time-varying or nonlinear capacitors. For example, take the case where the capacitor charge is a nonlinear function of the voltage. Then given the capacitor voltages, the currents are

$$I_c = \frac{d}{dt} Q_c = C(V_c)\,\frac{dV_c}{dt}$$

where $$Q_c = f_c(V_c) \tag{4}$$

and $$C(V_c) = \frac{df_c}{dV_c} \quad .$$

For this case, other indirect approaches have proved more fruitful.

Returning to equations (2) and (3), we observe that the average real power, P_k, and reactive power Q_k, absorbed by the capacitors at the frequency $\omega + k\omega_s$ are given by

$$P_k = \mathrm{Re}\left\{V^t_{c_k} I^*\right\}$$

$$Q_k = \mathrm{Im}\left\{V^t_{c_k} I^*\right\}$$

i.e., $$P_k + jQ_k = V^t_{c_k}\, I^*_{c_k} = -j(\omega+k\omega_s)N^t_{c_k}\, C\, N^*_{c_k} \tag{5}$$

where $V^t_{c_k}$ is the transpose of vector V_{c_k} and $I^*_{c_k}$ is the complex conjugate of vector I_{c_k}.

The Hermitian form $N_{c_k}^{t} C N_{c_k}^{*}$ is non-negative for positive capacitances. Hence, frequency-power formulas may be written as

$$\sum_{k=-\infty}^{\infty} P_k = 0 \tag{6a}$$

$$\sum_{k=-\infty}^{\infty} \frac{Q_k}{\omega+k\omega_s} \leq 0 \tag{6b}$$

where equation (6a) is satisfied trivially with $P_k \equiv 0$ for all k, simply stating that no real power is dissipated or generated by the capacitors at any of the frequencies $\omega + k\omega_s$.

Similarly, for the inductive subnetworks, let the inductor currents be given as

$$I_\ell = N_\ell(j\omega,t)e^{j\omega t} = \sum_{k=-\infty}^{\infty} N_{\ell_k}(j\omega)e^{j(\omega+k\omega_s)t} \tag{7}$$

Then the inductor voltages are

$$V_\ell = \sum_{k=-\infty}^{\infty} j(\omega+k\omega_s)L\, N_{\ell_k}(j\omega)e^{j(\omega+k\omega_s)t} \tag{8}$$

where

$$L = \text{diagonal } \{L_i\}$$

is the positive definite matrix of inductances.

The average real and reactive powers absorbed by the inductors at the frequency $\omega + k\omega_s$ are

$$P_k + jQ_k = V^t_{\ell_k} I^*_{\ell_k} = j(\omega+k\omega_s) N^t_{\ell_k} L N^*_{\ell_k} \tag{9}$$

We then obtain frequency-power formulas

$$\sum_k P_k = 0 \tag{10a}$$

$$\sum_k \frac{Q_k}{\omega+k\omega_s} \geqslant 0 \tag{10b}$$

Following the convention that reactive power absorbed by a capacitor is negative and reactive power absorbed by an inductor is positive, we note that equation (6) reduces to (10). But if by design, we have the following equation valid,

$$\sum_k N^t_{\ell_k} L N^*_{\ell_k} - \sum_k N^t_{c_k} C N^*_{c_k} = 0 \tag{11}$$

then frequency-power formulas may be written for the whole network as

$$\sum_k P_k = 0 \tag{12a}$$

$$\sum_k \frac{Q_k}{\omega+k\omega_s} = 0 \tag{12b}$$

where equation (12a) may be regarded simply as a statement of the principle of conservation of energy. Similarly, equation (12a), and hence equation (11), would indicate equal rates of absorption and generation of reactive power in the inductors and capacitors, respectively.

As noted by previous authors, the equations involving reactive powers do not lend themselves easily to physical interpretations, especially about the efficiency of real power-frequency conversion, which is of prime concern. Hence, in the next section, we shall take an external view of the SLC network to obtain non-trivial formulas involving the real power components.

4.2 Real Power Formulas

We now consider the SLC network with frequency selective terminations as shown in Fig. 4-2. Fig. 4-2(a) shows the more practical 4-terminal circuit with the SLC network coupling the source to the load. In Fig. 4-2(b), we have placed the source in parallel with the load, thus obtaining a 3-terminal circuit, and picture the SLC network as a 1-port in analogy with previous works on single nonlinear reactive or resistive elements.

As before, the current flowing out of the SLC network may be written in the form

$$I(j\omega,t) = y(j\omega,t)e^{j\omega t} \tag{13}$$

where $y(j\omega,t)$ is a transfer admittance function and is periodic in time with period T. Hence we can expand $I(j\omega,t)$ in the form

$$I = \sum_{k=-\infty}^{\infty} y_k(j\omega)e^{j(\omega+k\omega_s)t} \tag{14}$$

We may assume to start with that the tuning of each RLC series circuit is ideal so that each resistor dissipates power only at the center-tuned frequency. Then we have

$$I = \sum_k i_k(t)$$

where

$$i_k = y_k(j\omega)e^{j(\omega+k\omega_s)t} \tag{15}$$

Then

$$v_k = r_k i_k$$

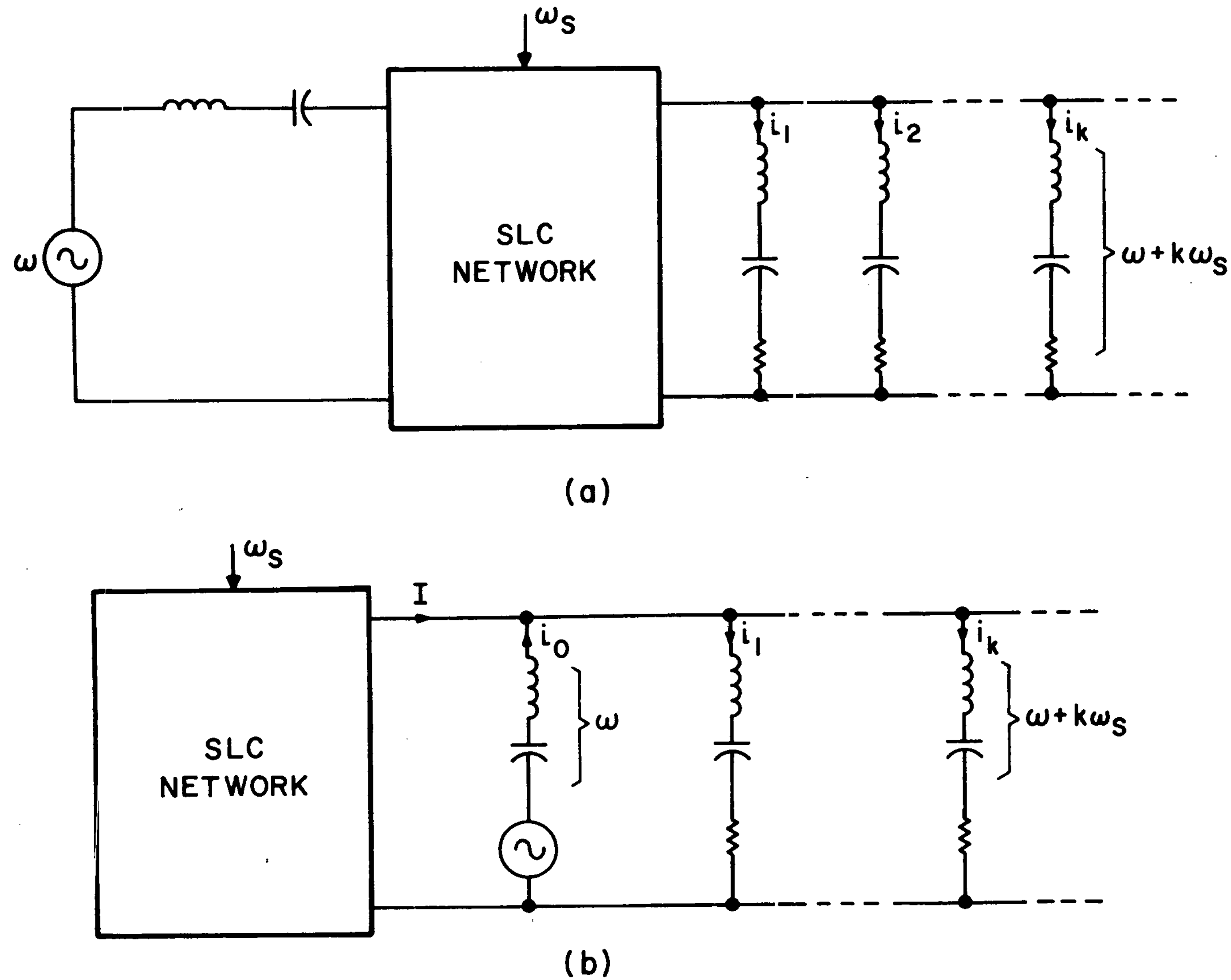

FIG. 4.2 SLC NETWORK WITH FREQUENCY-SELECTIVE LOAD

and hence the average real and reactive powers absorbed by the load at the frequency $\omega + k\omega_s$ are given by

$$P_k + jQ_k = V_k i_k^* = r_k \, |y_k(j\omega)|^2 \tag{16}$$

From the conservation of energy and the losslessness of the SLC network, we have the relation

$$-P_o + \sum_{k=1}^{\infty} P_k + \sum_{k=1}^{\infty} P_{-k} = 0 \tag{17}$$

where $$P_k = \mathrm{Re}\{V_k i_k^*\} = r_k \, |y_k(j\omega)|^2 \tag{18}$$

For a passive load, $r_k \geqslant 0$.

Hence, $P_k \geqslant 0$ and we have

$$-P_o + \sum_k k^2 P_k > 0 \tag{19}$$

In order to obtain information on conversion efficiencies using frequency-power formulas, it is commonly assumed that the form of the formulas is essentially unchanged when power is absorbed or supplied at only a finite number of frequencies. In particular when power is supplied at frequency ω and absorbed at only one frequency $\omega + k\omega_s$ equation (19) implies that

$$-P_o + k^2 P_k = h_k^2 \tag{20}$$

for some non-zero real number h_k.

Equation (20) gives a conversion efficiency

$$\eta = \frac{P_k}{P_o} = \frac{1}{k^2} + \frac{h_k^2}{k^2 P_o} \tag{21}$$

i.e.,

$$\eta > 1/k^2 \tag{22}$$

provided the trivial condition

$$P_k = P_o \equiv 0 \tag{23}$$

does not exist. As discussed in the next section, this result contrasts with Page's inverse square law of harmonic generation using positive nonlinear resistive elements which gives

$$\eta \lesssim 1/k^2 \tag{24}$$

To illustrate the contrast between SLC networks and ideal diode networks in the capability of the former to bypass Page's inverse square law, we consider the harmonic generator circuits shown in Fig. 4-3. In the steady state, with the appropriate phase relation between the source waveform and the operation of the douple pole-double throw switch, the voltage $v(t)$ is a full-wave rectified sine wave as given in Fig. 4-4(a). In contrast to the behavior of the diode bridge circuit shown in Fig. 4-3(b)[Page, 9], the current through the series RLC circuit of the SLC harmonic generator is independent of the charge on the capacitor so that in the steady state, it has a typical form as shown in Fig. 4-4(b). This may be demonstrated as follows:

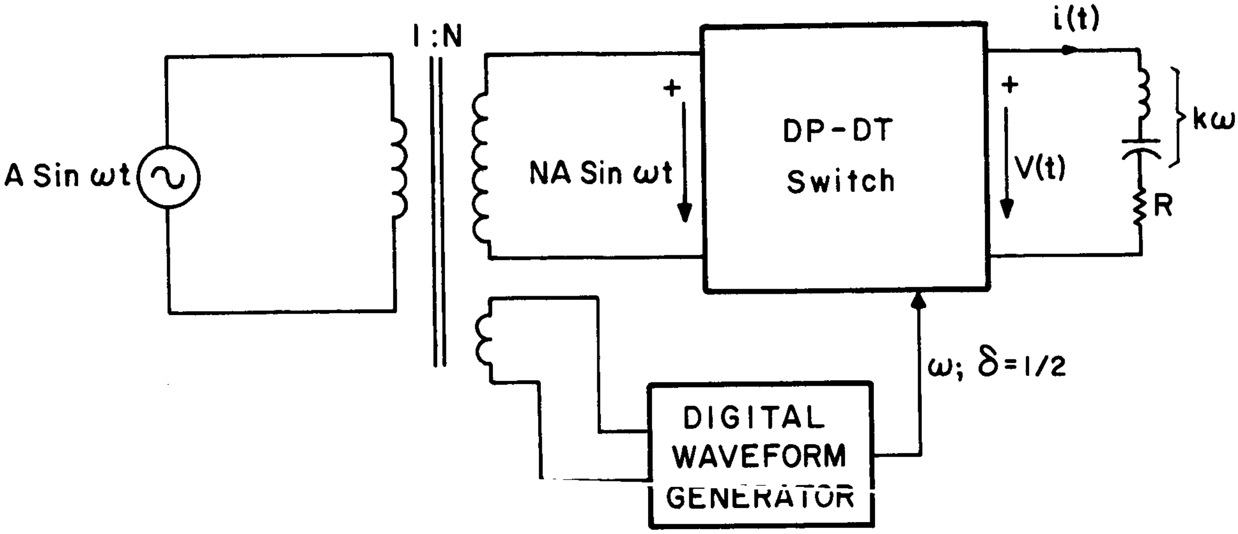

(a) SLC NETWORK

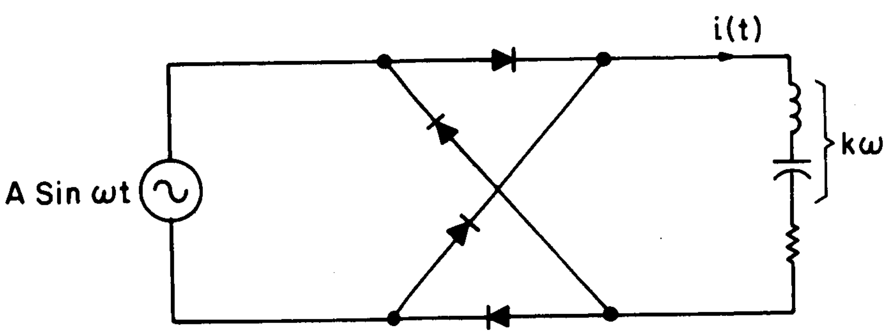

(b) BRIDGE-RECTIFIER CIRCUIT

FIG. 4.3 HARMONIC GENERATORS

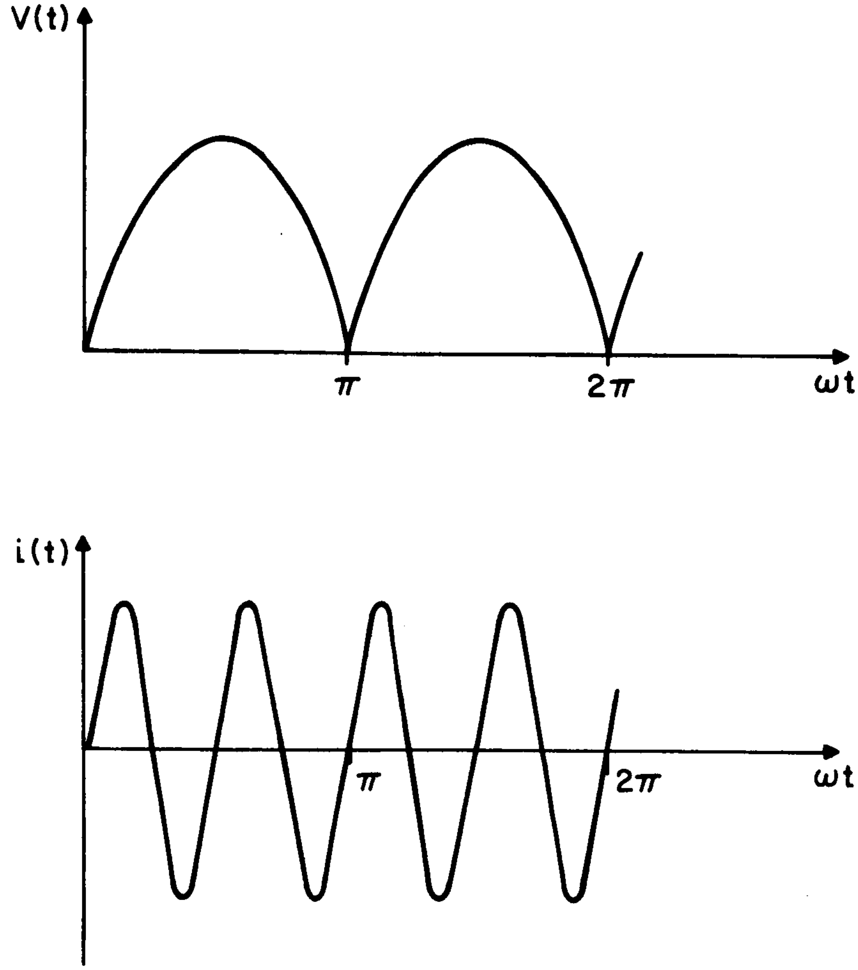

FIG. 4.4 TYPICAL WAVEFORMS FOR SLC HAMONIC GENERATOR

The coefficients of state equations for the SLC harmonic generator, shown without the transformer in Fig. 4-5 are related in the manner

$$A_1 = A_2 = A \ ; \ B_1 = -B_2 \ .$$

Hence $$E_1 = E_2 = A\text{-}pI = E$$

and the matrices Q_i, and vectors G_i are also related by:

$$Q_1 = Q_2 \ , \ Q = Q_1{}^2$$

$$G_1 = (I-Q_1)(pI-A)^{-1}B_1$$

$$G_2 = (I-Q_2)(pI-A)^{-1}B_2 = -G_1$$

Then, we also have

$$G = Q_2G_1 + G_2 = (Q_2-I)G_1$$

$$= -(I-Q_1)G_1$$

$$Z_1 = (I-Q)^{-1}G = -(I-Q_1{}^2)^{-1}(I-Q_1)G_1$$

$$= -(I+Q_1)^{-1}G_1$$

Similarly:

$$Z_2 = Q_1Z_1 + G_1 = -Q_1(I+Q_1)^{-1}G_1 + G_1$$

$$= \left[-Q_1(I+Q_1)^{-1} + I\right] G_1$$

$$= (I+Q_1)^{-1} \ (-Q_1+I+Q_1)G_1 = (I+Q_1)^{-1}G_1$$

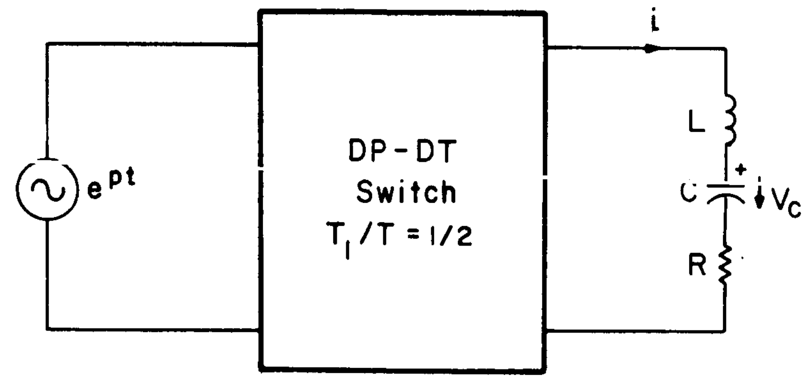

FIG. 4.5 SCHEMATIC DIAGRAM OF SLC HARMONIC GENERATOR

Hence $\quad Z_2 = -Z_1$.

The steady-state solution is given by

$$X(t)e^{-pt} = \begin{cases} e^{E(t-kT)}\left[Z_1+E^{-1}B_1\right] -E^{-1}B_1 \ , & t\in I_{1k} \\ e^{E(t-kT-T/2)}\left[-Z_1-E^{-1}B_1\right] + E^{-1}B_1 \ , & t\in I_{2k} \end{cases}$$

Now writing out the coefficients of the state-space equations explicitly, with

$$X = \begin{bmatrix} V \\ i \end{bmatrix}$$

we have

$$A = \begin{bmatrix} 0 & 1/C \\ -1/L & -R/L \end{bmatrix} \quad , \quad B_1 = \begin{bmatrix} 0 \\ 1/L \end{bmatrix}$$

Hence

$$(pI-A)^{-1} = \frac{1}{D(p)} \begin{bmatrix} p+2\alpha & 1/C \\ -1/L & p \end{bmatrix}$$

where $\quad D(p) = (p+\alpha)^2 + \beta^2$

and $\quad \alpha = \frac{R}{2L} \quad , \quad \beta^2 = \frac{1}{LC} - \alpha^2$.

Also, by Laplace transform inversion of $(pI-A)^{-1}$, we have

$$e^{At} = e^{-\alpha t}\begin{bmatrix} \text{Cos } \beta t + \frac{\alpha}{\beta} \text{ Sin } \beta t & \frac{1}{\beta C} \text{ Sin } \beta t \\ \\ -1/\beta L \text{ Sin } \beta t & \text{Cos } \beta t - \frac{\alpha}{\beta} \text{ Sin } \beta t \end{bmatrix} .$$

Then other quantities in the steady-state solution are obtained as follows:

$$Q_1 = e^{ET/2} = e^{-pT/2}\, e^{AT/2}$$

$$= (-1)^k\, e^{-(p+\alpha)T/2}\, I$$

for $\beta = \frac{2\pi k}{T}$, k a positive integer since harmonic generation is desired.

Also, $$G_1 = (I-Q_1)(pI-A)^{-1}B_1$$

$$= \frac{\left[1 - (-1)^k e^{-(p+\alpha)T/2}\right]}{D(p)} \begin{bmatrix} 1/LC \\ \\ p/L \end{bmatrix}$$

and $$Z_1 = -(I+Q_1)^{-1}G_1$$

$$= \frac{-\left[1 - (-1)^k e^{-(p+\alpha)T/2}\right]}{D(p)\left[1 + (-1)^k e^{-(p+\alpha)T/2}\right]} \begin{bmatrix} 1/LC \\ \\ p/L \end{bmatrix} .$$

Hence

$$Z_1 + E^{-1}B_1 = \frac{-2}{D(p)\left[1 + (-1)^k e^{-(p+\alpha)T/2}\right]} \begin{bmatrix} 1/LC \\ p/L \end{bmatrix} .$$

We then obtain the following exact expression for the steady-state current response during either time interval to the input e^{pt}.

$$i(t) = \frac{-2e^{-\alpha t}}{D(p)\left[1 + (-1)^k e^{-(p+\alpha)T/2}\right]} \left[\frac{p}{L} \operatorname{Cos} \beta t - \left(\frac{\alpha p}{\beta L} + \frac{1}{\beta L^2 C}\right) \operatorname{Sin} \beta t\right]$$

$$+ \frac{p}{L \cdot D(p)} e^{pt} .$$

Assuming that the tuning factor of the load may be arbitrarily increased so that power is dissipated only at the center frequency $k\omega_s$, we have

$$\alpha \to 0 \quad \text{so that} \quad e^{-\alpha T/2} \approx 1 - \alpha T/2 \quad \text{and} \quad \beta^2 \to 1/LC .$$

Then for a real sinusoidal input voltage of amplitude NA and frequency ω_s, the current through the series resistance is approximately sinusoidal, with frequency β and amplitude

$$\left(\frac{4NA}{\pi R}\right)\left(\frac{k}{k^2-1}\right)$$

for k even.

The power supplied to the load at the harmonic frequency $k\omega_s$ is

$$P_k = \begin{cases} \dfrac{8k^2N^2A^2}{\pi^2 R(k^2-1)^2} , & k \text{ even} \\ 0 , & k \text{ odd} \end{cases}$$

By selecting a transformer ratio

$$N = \frac{\pi(k^2-1)}{4k}$$

we have

$$P_o = P_k = \frac{A^2}{2R} \quad .$$

Thus the circuit of Fig. 4-4(a) is ideally capable of converting all available power at frequency ω to power at any even order harmonic frequency $k\omega$ with 100 per cent efficiency.

It may be noted that the expression for P_k may be obtained by Fourier analysis on the full-wave rectified voltage waveform and setting

$$P_k = \frac{|V_k|^2}{2R} \quad .$$

However, such an analysis does not illustrate the absence of the trivial condition, $P_o \equiv 0$.[e.g., see 11]

Also, an analysis similar to the above may be carried out with a tuned idle circuit in place of the ideal transformer, with the ratio of the center frequency of the idle circuit to the switching frequency, $r = \omega_i/\omega_s$ as the design parameter in place of the transformer ratio N.

4.3 Comparison of SLC Networks and Nonlinear Frequency Conversion Systems

Before discussing other practical aspects, we briefly review some results derived from the frequency-power formulas for nonlinear resistors and nonlinear reactors by previous workers.

The frequency-power formulas for positive nonlinear resistors with independent frequencies ω_1 and ω_2, and generated frequencies $m\omega_1 + n\omega_2$ are given by [Pantell, 3]:

$$\sum_{m=0}^{\infty} \sum_{n=-\infty}^{\infty} m^2 P_{mn} \geq 0 \tag{24a}$$

$$\sum_{m=-\infty}^{\infty} \sum_{n=0}^{\infty} n^2 P_{mn} \geq 0 \tag{24b}$$

The relations for nonlinear reactors under similar conditions are [Manley and Rowe, 2]:

$$\sum_{m=0}^{\infty} \sum_{n=-\infty}^{\infty} \frac{m\, P_{mn}}{m\omega_1 + n\omega_2} = 0 \tag{25a}$$

$$\sum_{m=-\infty}^{\infty} \sum_{n=0}^{\infty} \frac{n\, P_{mn}}{m\omega_1 + n\omega_2} = 0 \tag{25b}$$

where P_{mn} is the average real power absorbed by the nonlinear element at the frequency $m\omega_1 + n\omega_2$.. It should be noted that the sign convention for positive power in this section is the reverse of that used in the previous section, where a positive sign is associated with real power $P_k (k \geqslant 1)$ generated by an SLC network.

We consider two specific power/frequency conversion problems: harmonic generation and amplitude modulation.

Harmonic Generation: Suppose the nonlinear element is driven by only one source at frequency ω so that the generated frequencies are $n\omega$. Equations (24) and (25) then reduce to the single equations, respectively:

$$\sum_n n^2 P_n \geq 0 \tag{26}$$

$$\sum_n P_n = 0 \tag{27}$$

where P_n is the average real power absorbed by the nonlinear element at frequency $n\omega$.

If power is absorbed at only one frequency $n\omega$, then equation (26) predicts that the efficiency of generation of the n^{th} harmonic,

$$\eta = \left|\frac{P_n}{P_1}\right|$$

cannot exceed $1/n^2$.

With nonlinear reactors, from equation (27), the maximum efficiency is theoretically 100 per cent, independent of the order of the harmonic.

Amplitude Modulation. Suppose the nonlinear element is driven by two sources at frequencies ω_1 and ω_2 but power is absorbed at the output only at frequency $m\omega_1 + n\omega_2$. Equation (24) then reduces to

$$P_{10} + m^2 P_{mn} \geq 0$$

$$P_{01} + n^2 P_{mn} \geq 0$$

The conversion efficiency is then

$$\eta = \left| \frac{P_{out}}{P_{in}} \right| = \frac{|P_{mn}|}{|P_{01}+P_{10}|} \leq \frac{1}{m^2+n^2}$$

Under the same conditions, equation (25) reduces to

$$\frac{P_{10}}{\omega_1} + \frac{m\ P_{mn}}{m\omega_1+n\omega_2} = 0$$

$$\frac{P_{01}}{\omega_2} + \frac{n\ P_{mn}}{m\omega_1+n\omega_2} = 0$$

Hence $$\eta = \left| \frac{P_{out}}{P_{in}} \right| = \frac{|P_{mn}|}{|P_{01}+P_{10}|} = 1$$

Thus, for nonlinear reactors, the maximum conversion efficiency is 100 per cent, independent of m and n, whereas for nonlinear resistors, even with $m = n = 1$, i.e., for first upper sideband modulation, the maximum conversion efficiency is 50 per cent.

For SLC networks, there is no fundamental limitation on the efficiency of frequency conversion. Particularly, the discussion contained in the previous section implies that SLC networks are not constrained by Page's inverse square law. However, the expectation of 100 per cent efficiency in frequency conversion is not based on the condition of lossless coupling alone. As Page[9] has emphasized, the ideal diode with the voltage-current relation

$$vi = 0 \ , \ v \leq 0 \ , \ i \geq 0$$

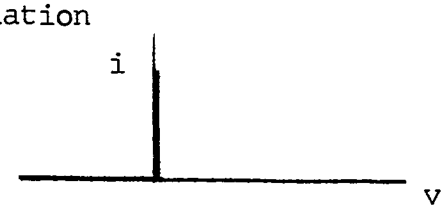

is lossless, but its efficiency for generation of the m^{th} harmonic cannot exceed $1/m^2$, no matter the ingenuity of the circuit configuration or filter design.

Similarly, for another common switching device, the single silicon controlled rectifier (SCR), the efficiency of generating the m^{th} harmonic is proportional to $1/m^2$; for, with a firing angle $\alpha < \pi$ and anode commutation taking place whenever the anode current attempts to reverse polarity, the m^{th} harmonic power is proportional to the square of the m^{th} Fourier coefficient of the output voltage waveform, and this is also an upper bound on the efficiency;

i.e., $\eta = | a_n^2 + b_n^2 |$

where

$$a_n = \frac{1}{\pi(n^2-1)} \left[n \operatorname{Cos} n\alpha \operatorname{Cos} \alpha + \operatorname{Sin} n \alpha \operatorname{Sin} \alpha + n(-1)^n \right]$$

$$b_n = \frac{1}{\pi(n^2-1)} \left[n \operatorname{Cos} n\alpha \operatorname{Sin} \alpha - \operatorname{Sin} n\alpha \operatorname{Cos} \alpha \right]$$

Hence

$$\eta = \frac{1}{\pi^2(n^2-1)^2} \Big[n^2+1 + (n^2-1)\operatorname{Cos}^2 n\alpha + (-1)^n n(n-1) \operatorname{Cos} (n+1)\alpha$$
$$+ (-1)^n n(n+1) \operatorname{Cos} (n-1)\alpha \Big]$$

This result reflects the intermediate nature of the SCR between the ideal diode and the ideal switch.

Thus the high values of efficiency which can be obtained when silicon controlled rectifiers are used in applications such as dc-dc converters and dc-ac inverters cannot be realized in ac-ac converters directly.

From the discussion in this and the previous section, we note, in summary, the characteristics which enable the ideal switch to bypass Page's Law as follows:

(1) the fundamental characteristic is the ability to switch ON and OFF at arbitrary instants independent of the instantaneous amplitudes and phases of the voltages and currents in the circuit;

(2) a second property, which is necessary for the operation of the circuit shown in Fig. 4-3(a) but is not fundamental, is the bidirectional capability, i.e., when OFF, it blocks both positive and negative currents and when ON, it conducts current in either direction depending upon the state of the rest of the circuit.

The main advantage of SLC networks over nonlinear reactive elements capable of operating at comparable power and frequency levels, such as saturable core reactors is in the potential compactness of the former, as with all solid-state technology. The disadvantage, at the current state of the art, is that the ideal switch is not available as an integral unit, but can only be

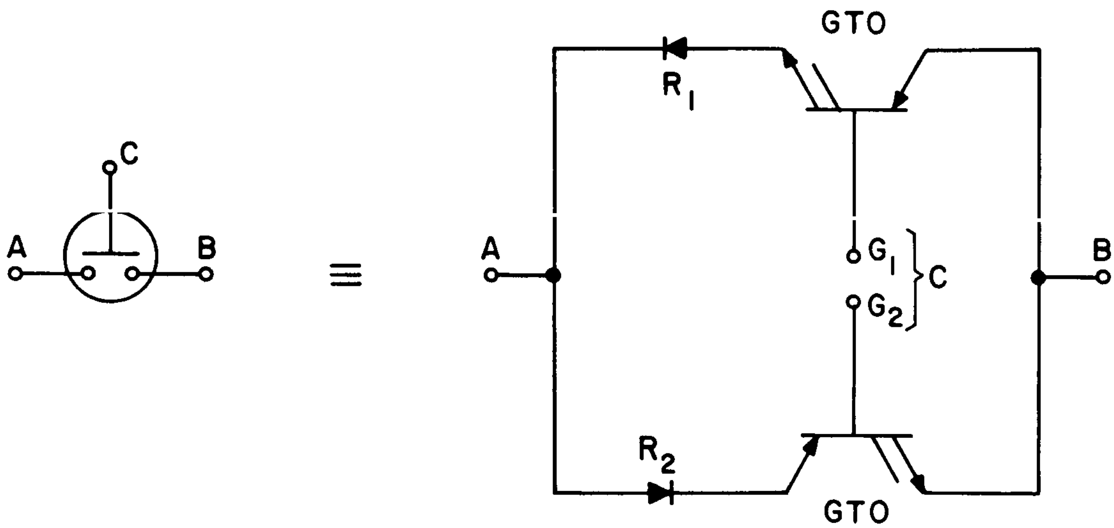

FIG. 4.6 SIMULATION OF IDEAL SWITCH

simulated by the connection of two power transistors or gate-turn off switches in inverse parallel as shown in Fig. 4-6.

The rectifiers R_1 and R_2 are for protection of the active devices for possible extension of the operating power levels.

Even though the ideal switch is not currently available as a single unit, its stipulation is in step with the trend in solid-state device integration and design as represented by the advances from the basic SCR units to triacs and gate-turn off switches in the last decade. [See Appendix for brief description of these devices.]

References for Chapter 4

1. Penfield, P., Jr., Frequency-Power Formulas, MIT Press and J. Wiley and Sons, N.Y., 1960.
2. Manley, J.M. and Rowe, H.E., "Some General Properties of Non-linear Elements, part 1: General Energy Relations," Proc. IRE, Vol. 44, pp. 904-913, July 1956.
3. Pantell, R.H., "General Power Relationships for Positive and Negative Non-Linear Resistive Elements," Proc. IRE, Vol. 46, No. 12, pp. 1910-1913, Dec. 1958.
4. (a) Page, C.H., "Frequency Conversion with Positive Nonlinear Resistors," J. Res. Natl. Bur. Stand., Vol. 56, pp. 179-182, April 1956.
4. (b) Page, C.H., "Frequency Conversion with Nonlinear Reactance," J. Res. Natl. Bur. Stand., Vol. 58, No. 5, pp. 227-236, May 1957.
5. Bennett, W.R., "Amplification in Nonlinear Reactive Networks," Proc. of the Symposium on Active Networks and Feedback Systems, Polytechnic Institute of Brooklyn, pp. 645-658, April 1960.
6. Duinker, S., "General Properties of Frequency Converting Networks," Philips Research Reports, Vol. 13, pp. 37-78, 101-148, 1958.
7. Della Torre, E. and Sirkis, M.D., "Power Conversion with Nonlinear Reactances," IRE Trans. on Circuit Theory, Vol. CT-8, pp. 95-99, June 1961.
8. Snelsire, R.W. and Finzi, L.A., "Power Transfers in Nonlinear Frequency Converters with Three Commensurable Frequencies," IEEE Trans. on Magnetics, Vol. MAG-1, pp. 53-56, March 1965.

9. Page, C.H., "Harmonic Generation with Ideal Rectifiers, Proc. IRE, Vol. 46, No. 10, pp. 1738-1740, Oct. 1958.

10. Black, W.L., "Some New Power-Frequency Inequalities for Non-linear Capactive Harmonic Multipliers," Proc. IEEE, Vol. 54, pp. 1995-1996, Dec. 1966.

11. Tucker, D.G., "Highly-Efficient Generation of a Specified Harmonic or Subharmonic by Means of Switches," The Radio and Electronic Engineer, Vol. 28, pp. 25-32, July 1964.

Chapter 5: MODELLING OF LINEAR TIME VARYING SYSTEMS

5.1 Introduction

The problem of synthesis and modelling of linear time-varying networks and systems has received a great deal of attention in recent years.[1,2] One commonly used approach is to obtain a system described by a set of state equations of the form

$$\dot{x} = A(t)x(t) + B(t)u(t)$$
$$y(t) = C(t)x(t) \tag{1}$$

for which a given matrix $H(t,\tau)$ is the impulse response matrix. The state equations (1) may then be used in an analog simulation of the given network or system.

The other approach is to realize input-output specifications by using networks of a restricted class of elements connected in a specific manner, as in classical network synthesis. Meadows et alia[3] utilize a canonical n-path network with analog signal generators and multipliers, constituting amplifiers with time-varying gains, as the only time-varying elements. Spaulding and others[4,5] utilize time-varying multiport gyrators and transformers terminated in unit fixed elements.

In practice the analog waveforms required in the n-path realization are complicated and difficult to generate, while realizations of a single time-varying gyrator or transformer requires many active elements and much design effort.[6]

On the other hand, only a small number of devices are required for realization of an ideal switch, and the waveforms required for switching are digital and hence more easily generated. Thus, we can expect some practical advantages in modelling linear time-varying systems using only ideal switches as the time-varying elements.

In this chapter, we consider specifically the problem of realizing a given function $Y(p,t)$ as the driving point admittance function of a periodically time-varying, lossless network. The admittance function is defined by the relation

$$I(p,t) = Y(p,t)e^{pt} \tag{2}$$

where $I(p,t)$ is the current flowing into the network at the input port and e^{pt} is the driving point voltage waveform, as shown in Fig. 3-4. As discussed in Chapter 3, $Y(p,t)$ is periodic in time with period T equal to the period of the time variation of the network. When $Y(p,t)$ is not specified directly, it may be derived from the impulse response by the integral transform

$$\begin{aligned} Y(p,t) &= \int_0^\infty H(t,t-\xi)e^{-p\xi}\, d\xi \\ &= \int_{-\infty}^{t} H(t,\tau)e^{-p(t-\tau)}\, d\tau \end{aligned} \tag{3}$$

where $H(t,\tau)$ is the current into the network at the input port for a voltage impulse applied at time $t = \tau$.

Two other necessary conditions that must be satisfied by the driving point admittance function, $Y(p,t)$, of a lossless network are:

1. the pole locations are time-invariant and all lie on the imaginary axis:

$$P_{ki} = j(\omega_i + k\omega_s), \; i = 1, \ldots n \; ; \; k = 0, \pm 1, \ldots \tag{4}$$

where

$$\omega_s = 2\pi/T$$

2. the time-average of the real part of $Y(j\omega,t)$ is zero:

$$\langle \mathrm{Re}\{Y(j\omega,t)\}\rangle = 0 \tag{5}$$

5.2 Approximation and Design of Driving Point Functions

In this section, we consider the problem of designing a given driving point function of a periodically time-varying lossless network by means of SLC networks. As is well-known, any passive driving point function may be realized by terminating a certain derived lossless network by a unit resistor, so that the realization of lossless networks is basic to the whole network realization problem.

Suppose we are given a system in the form (1), with coefficients A(t), B(t), C(t) all periodic in time with a common period T. A step that naturally presents itself is to approximate all the time-varying coefficients with a finite number of piecewise constant matrices over a period $kT \leqslant t \leqslant (k+1)T$. For example, A(t) may be replaced, over a period, by

$$A(t) \cong \sum_{i=1}^{n} A(t_i) \left[u(t-t_i) - u(t-t_{i+1})\right] \tag{6}$$

and similarly for B(t) and C(t), with the set $\{t_i\}$ chosen in an appropriate manner.

Let

$$A_i = A(t_i) \ , \ T_i = t_{i+1} - t_i$$

where

$$\sum_{i=1}^{n} T_i = T \ .$$

Divide the time interval $kT \leqslant t \leqslant (k+1)T$ into n sub-intervals

$$I_{ik} : kT + T_{i-1} \leqslant t \leqslant kT + T_i \;, \; i = 1, \ldots n.$$

Then the state-space equations can be written approximately in the form

$$\left.\begin{aligned} \dot{x}(t) &= A_i x(t) + B_i u(t) \\ y(t) &= C_i x(t) \end{aligned}\right\} t \in I_{ik}, \; i = 1,2,\ldots n \tag{7}$$

Considering the describing differential equations alone, the system (7) may be simulated by the commutated n-path network of Fig. 5-1, and if each path is an SLC network, then the whole system is lossless. However, the network is not appropriate for design of input-output system functions because of the difficulties of taking account of boundary conditions at transitions from one path to the other and keeping the poles of the steady-state system functions time-invariant at pre-assigned locations. To find modifications needed to overcome these difficulties, let us consider in detail the 2-path case. The normal form equations may be written as

$$\left.\begin{aligned} \dot{x}_1 &= A_{11} x_1 + B_1 u(t) \\ \dot{x}_2 &= A_{21} x_2 \\ y &= C_1 x_1 \end{aligned}\right\} t \in I_{1k} \tag{8}$$

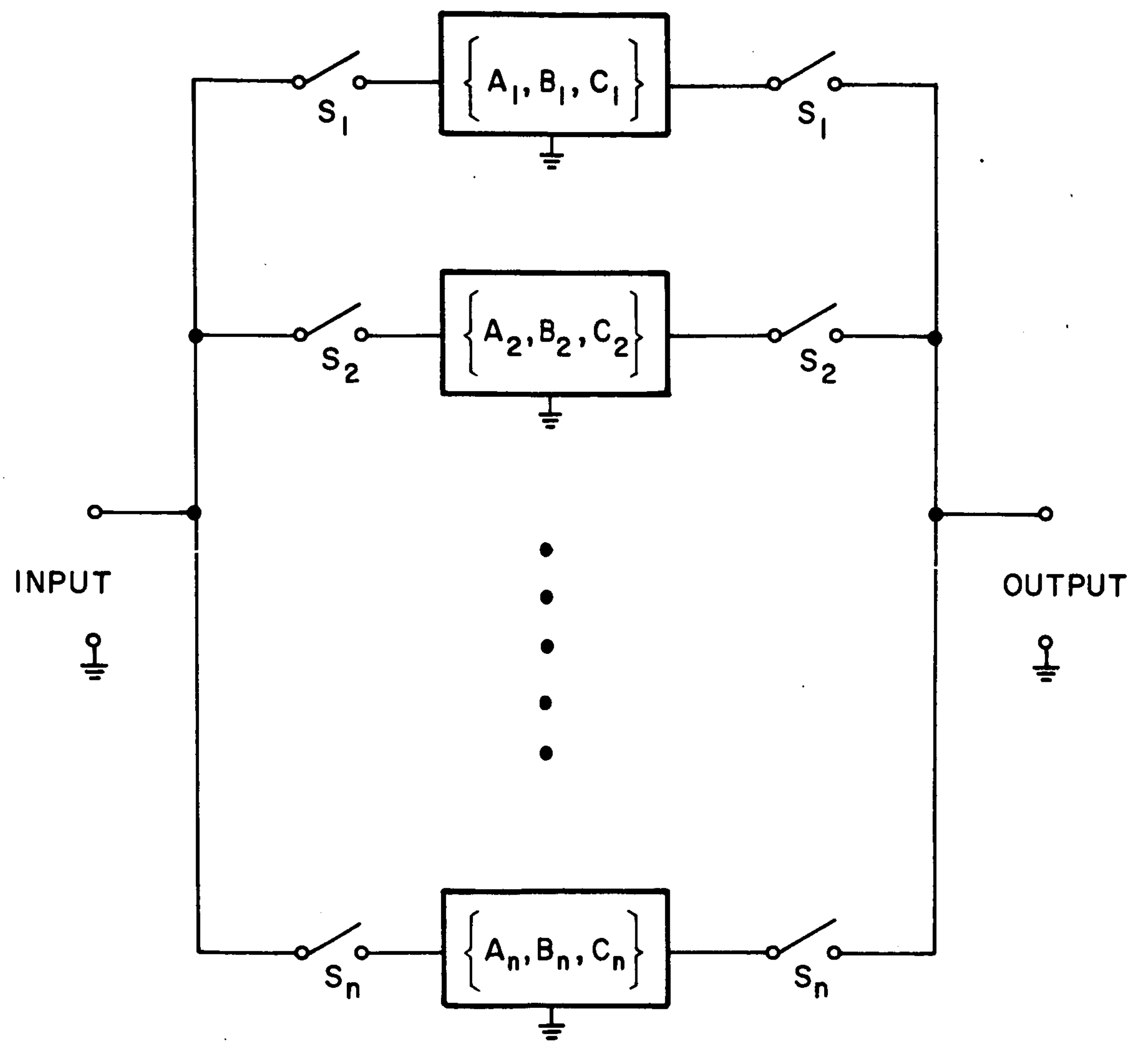

FIG. 5.1 COMMUTATED n-PATH NETWORK

and

$$\left.\begin{aligned} \dot{x}_1 &= A_{12}x_1 \\ \dot{x}_2 &= A_{22}x_2 + B_2u(t) \\ y &= C_2x_2 \end{aligned}\right\} t \in I_{2k} \tag{9}$$

As in Chapter 2, let $u(t) = e^{pt}$,

and

$$Z_i = x_i e^{pt}$$

$$E_{ij} = A_{ij} - pI \,, \tag{10}$$

we then have the transformed equations

$$\left.\begin{aligned} \dot{Z}_1 &= E_{11}Z_1 + B_1 \\ \dot{Z}_2 &= E_{21}Z_2 \end{aligned}\right\} t \in I_{1k} \tag{11}$$

and

$$\left.\begin{aligned} \dot{Z}_1 &= E_{12}Z_1 \\ \dot{Z}_2 &= E_{22}Z_2 + B_2 \end{aligned}\right\} t \in I_{2k} \tag{12}$$

The solutions of these equations are

$$\left.\begin{aligned} Z_1(t) &= e^{E_{11}(t-kT)} Z_1(kT) + \left[e^{E_{11}(t-kT)} - I \right] E_{11}^{-1} B_1 \\ Z_2(t) &= e^{E_{21}(t-kT)} Z_2(kT) \end{aligned}\right\} t \in I_{1k} \tag{13}$$

and

$$\left.\begin{aligned} Z_1(t) &= e^{E_{12}(t-kT-T_1)} Z_1(kT+T_1) \\ Z_2(t) &= e^{E_{22}(t-kT-T_1)} Z_2(kT+T_1) + \left[e^{E_{22}(t-kT-T_1)} - I\right] E_{22}^{-1} B_2 \end{aligned}\right\} t \in I_{2k} \tag{14}$$

The continuity of $Z_1(t)$ and $Z_2(t)$ at the switching instants provide, in the steady state, the solutions

$$Z_{1ss}(kT) = \left(I-Q_1\right)^{-1} G_1 \tag{15a}$$

$$Z_{1ss}(kT+T_1) = Q_{11} Z_{1ss}(kT) + G_{11} \tag{15b}$$

$$Z_{2ss}(kT) = \left(I-Q_2\right)^{-1} G_2 \tag{15c}$$

$$Z_{2ss}(kT+T_1) = Q_{21} Z_{2ss}(kT) \tag{15d}$$

where the Q and G matrices are defined as follows

$$\left.\begin{aligned} Q_{11} &= e^{E_{11}T_1}, \quad Q_{12} = e^{E_{12}T_2}, \quad Q_1 = Q_{11}Q_{12} \\ Q_{21} &= e^{E_{21}T_1}, \quad Q_{22} = e^{E_{22}T_2}, \quad Q_2 = Q_{21}Q_{22} \\ G_{11} &= \left(e^{E_{11}T_1} - I\right) E_{11}^{-1} B1 \\ G_{22} &= \left(e^{E_{22}T_2} - I\right) E_{22}^{-1} B_2 \\ G_1 &= Q_{12}G_{11} \\ G_2 &= Q_{21}G_{22} \end{aligned}\right\} \tag{16}$$

The desired steady-state system function is then given by

$$H(p,t) = \begin{cases} C_1Z_1(p,t) \ , & t\in I_{1k} \\ \\ C_2Z_2(p,t) & t\in I_{2k} \end{cases} \tag{17}$$

We observe that for the poles of H(p,t) not to have residue functions that are zero over a finite time interval, we must have the relations

$$\det\left[I-Q_1\right] = \det\left[I-Q_2\right] = 0 \tag{18a}$$

$$\det\left[E_{11}\right] = \det\left[E_{22}\right] = 0 \tag{18b}$$

satisfied at the same values of p.

A basic structure for which equation (22) holds is the 2-path, 2nd order network shown in Fig. 5-2, where

$$A_{11} = A_{12} = \begin{bmatrix} 0 & -1/L_1 \\ \\ 1/C_1 & 0 \end{bmatrix} , \ B_1 = \begin{bmatrix} 1/L_1 \\ \\ 0 \end{bmatrix} \tag{19a}$$

$$A_{21} = A_{22} = \begin{bmatrix} 0 & -1/L_2 \\ \\ 1/C_1 & 0 \end{bmatrix} , \ B_2 = \begin{bmatrix} 1/L_2 \\ \\ 0 \end{bmatrix} \tag{19b}$$

and

$$L_1C_1 = L_2C_2 \tag{20}$$

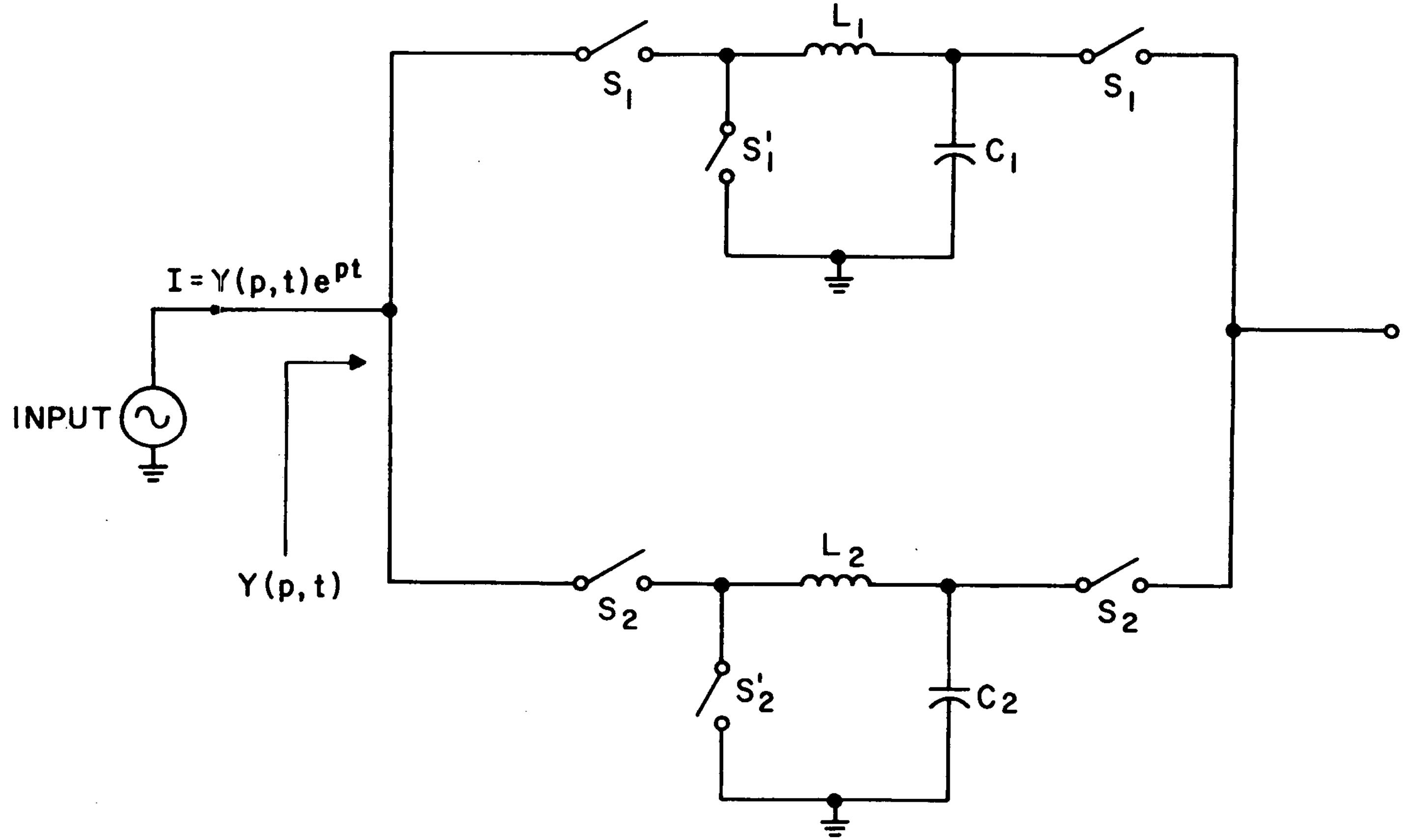

FIG. 5.2 BASIC 2nd ORDER, 2-PATH SLC NETWORK

For this case,

$$x_i = \begin{bmatrix} i_{L_i} \\ V_{C_i} \end{bmatrix} \quad , \quad i = 1, 2 .$$

Hence the input current is

$$I = \begin{cases} i_{L_1} \quad , \quad t \in I_{1k} \\ i_{L_2} \quad , \quad t \in I_{2k} \end{cases}$$

Since $i_{L_i} = C^t x_i$, for $C = \begin{bmatrix} 1 \\ 0 \end{bmatrix}$, the driving point admittance function is

$$Y(p,t) = \begin{cases} C^t Z_1(p,t) \quad , \quad t \in I_{1k} \\ C^t Z_2(p,t) \quad , \quad t \in I_{2k} \end{cases} \tag{21}$$

This network realizes one of the frequencies $\{\omega_i\}$ denoted in equation (4), so that to realize all n basic pole locations, n basic 2nd order-two-path structures may be connected in parallel, as in Fig. 5-3. Note that in Fig. 5-3, we have included a series connection of the capacitor voltages by means of a multi-winding transformer. This connection does not affect the driving point characteristics, but indicates a logical step in the extension of the procedure to 2-port system function realizations.

From the expressions for $Z_1(p,t)$ and $Z_2(p,t)$ in (13) and (14), we observe that the variation of the residue function during the time intervals I_{1k} and I_{2k} is determined by the location of the pole. Thus, even though the residue function is periodic in time with the

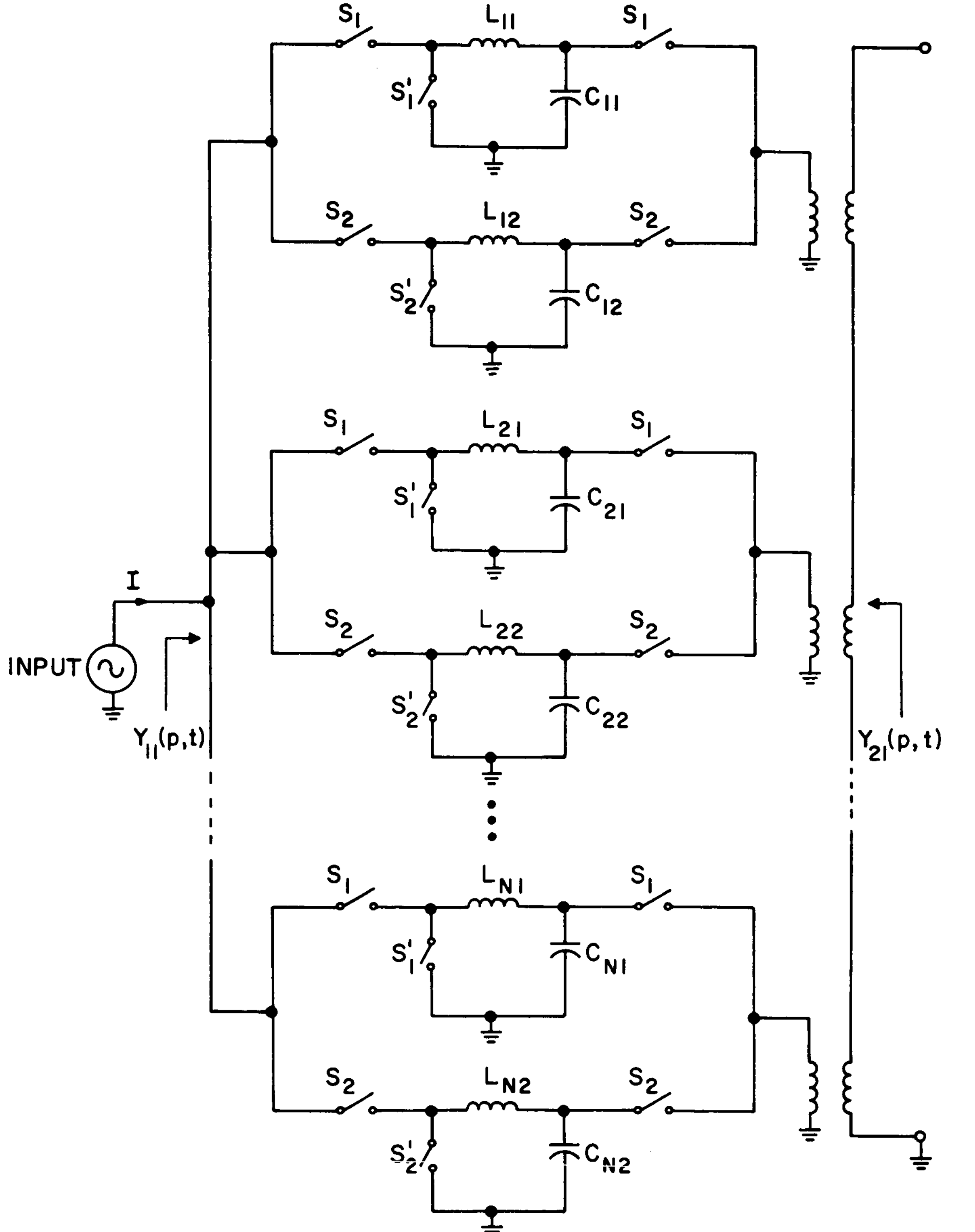

FIG. 5.3 PARALLEL CONNECTION OF BASIC 2-PATH, 2nd ORDER SLC NETWORKS TO REALIZE $Y_{11}(p,t)$

required period of the time variation of the network (equal to the period of operation of the switches), it is not possible to realize exactly the continuous time variation of the residue function. This limitation is due to the discontinuous nature of the switch. However, to approximate an arbitrary residue function within acceptable tolerances, several design parameters are available:

(1) The amplitude of oscillation of the residue functions in either time interval I_{1k}, I_{2k} may be arbitrarily changed by changing the ratios $\frac{L_i}{C_i}$ while keeping the products L_iC_i constant.

(2) Either the duty cycle of the operation of the switches may be changed or the number of paths of basic 2nd order networks may be arbitrarily increased if necessary.

However, we shall not carry this consideration further, but instead, we shall give an example to illustrate the explicit form of the residue function.

Example: Realize a driving point admittance function with poles located at the points

$$P_k = j(1 + k/2) \ , \ k = 0, \pm 1, \pm 2, \ldots$$

Hence $\omega_1 = 1 \ , \ \omega_s = 1/2 \ , \ T = 4\pi$.

We select the values $L_1 = L_2 = 1h$, $C_1 = C_2 = 1f.$ and $^{T}1/T = 1/2$. Then the admittance function is given explicity by:

$$Y(p,t) = \begin{cases} Y_1(p,t-kT) \ , & kT < t < kT + T/2 \\ Y_2(p,t-kT-1/2\ T) \ , & kT + T/2 < t < (k+1)T \end{cases}$$

where

$$Y_1(p,t) = \frac{-(1-e^{-2\pi p})e^{-pt}(p \text{ Cos } t - \text{Sin } t)}{(p^2+1)(1-e^{-4\pi p})} + \frac{p}{p^2+1}$$

$$Y_2(p,t) = \frac{-(1-2e^{-4\pi p} + e^{-6\pi p})e^{-pt}(p \text{ Cos } t - \text{Sin } t)}{(p^2+1)(1-e^{-4\pi p})} + \frac{p}{p^2+1} \quad .$$

References for Chapter 5

1. Silverman, L. M., "Synthesis of Impulse Response Matrices by Internally Stable and Passive Realizations", IEEE Trans. on Circuit Theory, Vol. CT-15, Sept. 1968, pp. 239-245.
2. Anderson, B. D. and Moore, J. B., "Procedures for Time Varying Impedance Synthesis", Proc. 11th Midwest Symposium on Circuit Theory, May 1968, pp. 17-26.
3. Meadows, H. E., L. M. Silverman and L. E. Franks, "A Canonical Network for Periodically Variable Linear Systems", Proc. 1966 4th Allerton Conf. on Circuit and Systems Theory, pp. 649-658.
4. Spaulding, D. A., "Passive Time Varying Networks", Ph.D. Thesis, Stanford University, Stanford, Calif., January 1965, Chapter IV.
5. Spaulding, D. A., "Lossless Time-Varying Impedance Synthesis", Electronics Letters, Vol. 1, No. 6, Aug. 1965, pp. 165-168.
6. Rao, T. N. and Newcomb, R. W., "Direct-coupled Gyrator Suitable for Integrated Circuits and Time Variation", Electronics Letters, Vol. 2, No. 7, p. 250, July 1966.

CHAPTER 6: CONCLUSION

6.1 Summary of Results

In this thesis, we have carried out a study of a class of periodically time-varying lossless networks. These networks are made up of ideal capacitors, inductors and switches. The lossless condition is achieved by identifying potentially lossy situations and limiting the class of networks to exclude those cases where loss might occur when the switches are operated periodically. A complete state-space solution is given for a canonical subclass characterized by possession of a minimal number of reactive elements, a proper tree, and a state-vector which completely describes the network during both time intervals of constant state coefficients. An extension of the analysis is outlined for the case where the state vectors are not identical in the two time intervals, but are related by a constant nonsingular transformation.

Steady-state time-varying system functions are defined in a manner analogous to the treatment of time-invariant LC networks without imposing the condition of asymptotic stability. This is done by the choice of a particular set of initial conditions for which no aperiodic transient is launched. The system function vector $N(p,t)$ thus derived has properties consistent with the system functions of lumped periodically time-varying networks. It is periodic in time with period equal to that of the time variation of the elements of the network, in this particular case equal to the period of operation of the switches. Its pole locations are time-invariant and lie on the imaginary axis of the p-plane. For one-port networks, the imposition of the lossless condition gives the result that the time-average of the real parts of the driving point immittance functions are zero. For two-port networks with a passive time-invariant load, the lossless conditions leads to a relation between driving point and transfer immittances. For example, when the load is a one-ohm resistance, the time-average of the real part of the driving point admittance $Y_{11}(j\omega,t)$ is equal to the time-average of the square of the magnitude of the transfer admittance $Y_{21}(j\omega,t)$. These relations are observed to be extensions of familiar frequency domain properties of LC network driving point and transfer immittance functions.

Various frequency-power relations are derived for the class of networks. The relations involving reactive powers are mostly of theoretical interest only, indicating the fact that frequency conversion occurs only in the switches and not in the linear reactive elements. The relations involving real power indicate the absence of a fundamental upper bound on the efficiency of conversion. This contrasts with Page's inverse square law of harmonic generation using positive nonlinear resistors. However, since nonlinear reactors are also theoretically capable of 100 per cent efficiency in frequency conversion, the only advantage of the ideal switch over currently available elements such as saturable core reactors is likely to be the potential compactness of the ideal switch, at comparable power levels and frequency ranges. To realize this advantage, a solid state circuit for simulating the ideal switch is suggested, consisting of two gate-turn off switches connected in parallel and opposite direction of conduction.

Finally, the problem of realizing the system functions of linear time-varying networks using only ideal switches as time-varying elements is considered briefly. For the fundamental case of the driving point admittance function of a lossless, periodically time-varying one-port network, a suitable network consisting of sequentially commutated 2-path, 2nd order networks is selected and analyzed. This analysis shows that the poles of a given admittance function can be realized exactly, but the residue function, while appropriately periodic in time with the period of the switch, cannot be realized exactly in general. Parameters available for piecewise design of the residue function are the ratios of inductance values to capacitance values for each path, the duty cycle of the commutation and the number of paths to be used for each basic pole location.

6.2 Suggestions for Further Research

The results of this study may be classified into two groups as follows. The first group consists of the mathematical characterization of SLC networks and their circuit theoretical properties as a class of linear time-varying networks. The other group is concerned with the consequences of postulating the ideal switching element in the theory of electrical power conversion. Both types of results are necessary steps towards the broad goal of synthesizing time-varying circuits for electrical power processing (similar to the synthesis of communication networks), and the possibility of realizing these circuits using SLC networks. For example, in the circuit shown in Fig. 6-1, we have an available source of power, the voltage source $e^{j\omega t}$, and a voltage $k\, e^{j10\omega t}$ is desired across a resistive load of one ohm.

The currents at ports 1 and 2 are

$$I_1 = Y_{11}(j\omega,t)e^{j\omega t}$$

$$I_2 = Y_{21}(j\omega,t)e^{j\omega t} = k\, e^{10j\omega t}$$

Hence

$$Y_{21}(j\omega,t) = k\, e^{j9\omega t}$$

Also

$$\langle \mathrm{Re}\{Y_{11}(j\omega,t)\}\rangle = \langle |Y_{21}(j\omega,t)|^2\rangle = k^2$$

A possible selection of $Y_{11}(j\omega,t)$ may be

$$Y_{11}(j\omega,t) = k^2 e^{j9\omega t} + k^2$$

$$= k^2 \left[1 + e^{j9\omega t}\right] .$$

Then the power processing problem is reduced to that of synthesizing a lossless time-varying 2-port network which has the specified input and transfer admittance functions when terminated at port 2 with a resistive load of one ohm.

A complete solution of this problem requires further work on the realization and synthesis of time-varying 2-port networks, particularly lossless networks, for which the contents of Chapter 5 may serve as a starting point. Also, further work on the mathematical characterization of general power processing circuits in terms of time-varying system functions will complement the synthesis effort in the achievement of the desired goal.

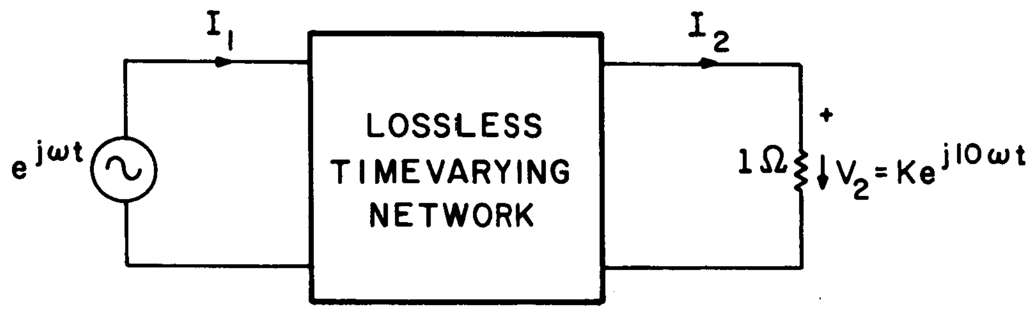

FIG. 6.1 SYNTHESIS OF POWER-PROCESSING CIRCUIT

APPENDIX

SOLID-STATE CONTROLLED SWITCHING DEVICES[1-3]

The purpose of this appendix is to discuss briefly the characteristics and parameters of some currently available solid-state controlled switching devices so as to place in perspective the properties of the ideal switch stipulated in the body of the thesis. The devices we shall consider specifically are the common two-junction, three layer transistor, the three-junction, four-layer silicon controlled rectifier (SCR) and two outgrowths of the SCR, the triode ac switch (triac) and the gate turn-off switch (GTO). These devices will be compared with respect to the following switching parameters:

(1) The maximum forward and reverse voltages that the device can block in its OFF state without avalanche break-down and conduction.

(2) The forward current rating and the forward voltage drop at rated forward current.

(3) The ratios of anode-cathode power to the gate turn-on power, and the gate turn-off power when this is applicable. [Often the switching sensitivity parameter is specified in terms of current ratios only.]

(4) The turn-on and turn-off times (switching speed).

The significance of some of these parameters are apparent; others require a brief explanation. The maximum forward and reverse blocking voltages limit the voltage level in the circuit in which a particular switching device may be utilized. Since devices are available for which these parameters may vary from hundreds of volts to 1KV or more, it might appear at first that they are not strong constraints on device selection. However, this is only partially true because in general, all the switching parameters are physically interrelated in such a way that improvement in one leads to degradation in one or more of the others. A good example of such a relation is that between the rated forward current and the turn-off time: the higher the forward current rating, the longer the turn-off time due to the finite rate of recovery and charge transfer in the various layers of the devices. The switching speed of a device, specified as the turn-on and turn-off times, limit the frequency ranges over which circuits using the device can operate. In the ideal switch, we postulated instantaneous change of state so that both the turn-on and turn-off times are zero. In the practical cases where these quantities have non-zero values, the maximum frequency of operation must be limited to values much less than $1/(t_{ON} + t_{OFF})$ Hz where t_{ON} and t_{OFF} are the turn-on and turn-off times, in seconds.

The forward voltage drop at rated forward current is a measure of the power loss in the switch in its ON state (for the ideal switch this is assumed to be zero); this limits the efficiency of power processing circuits. Another source of loss and efficiency limitation is the power required at the control gate to turn on the device from its blocking state and to turn it off from the conducting state when gate turn-off is possible. Hence a large value for the ratio of the power in the main anode-cathode channel to control gate power is desirable such that the gate power is negligible compared to the anode power as for the ideal switch.

Turning to actual devices, we note that the common transistor possesses the fundamental property of the ideal switch, i.e., it can be turned ON and OFF by the application of positive and negative control signals at the base-emitter terminals (given polarity of control signals are those for an n-p-n transistor and are reversed for a p-n-p transistor). The transistor is limited by its relatively low blocking voltages (less than several hundred volts), low switching sensitivity and long switching times, especially at higher power levels. Also, base current is required during the entire period of time when the transistor is in the ON state because it has no latching action. This further increases the gate power dissipation of the transistor switch. Typical switching parameters for power transistors are: blocking voltage of 100 volts; gate current sensitivity of 10 at rated collector current of 5 amps. and switching times in hundreds of microseconds, most of which is turn-off time.

To overcome some of the shortcomings of the transistor as a power switch, especially in the direction of higher blocking voltages, several four-layer p-n-p-n devices have been constructed. The most common of these for power applications is the silicon controlled rectifier (SCR) whose structure, symbol and typical V-I characteristics are shown in Fig. A-1. The higher blocking voltages (up to 1KV or more) are due to the additional, wider n-region, while the latching action which keeps the device conducting without the necessity of a continuous gate signal permits the use of pulsed control so that gate dissipation is reduced considerably. Thus the average turn-on current gain may be of the order of several thousands. The SCR also has fast switching speed with turn-on times of the order of one microsecond and turn-off times of tens of microseconds. Its main disadvantage is that once conducting, it cannot be turned off from the gate circuit, but only by a commutating action in the anode-cathode circuit that reduces the anode current to below the holding level.

Two outgrowths of the p-n-p-n device principle are the triac and the gate turn-off switch (GTO). The triac consists essentially of two SCR's connected in inverse parallel ("back-to-back") so that it can conduct in both directions of current flow in response to a positive or negative gate signal. Its operation and switching parameters are similar to those of the single SCR, except that it must be turned off only during the brief period while the load current is passing through zero; this limits the frequency of operation to less than 100 Hz for presently available triacs.

The GTO is another p-n-p-n device similar to the SCR, except its construction is such that it can be turned off by the application of a negative gate current. However, the turn-off current

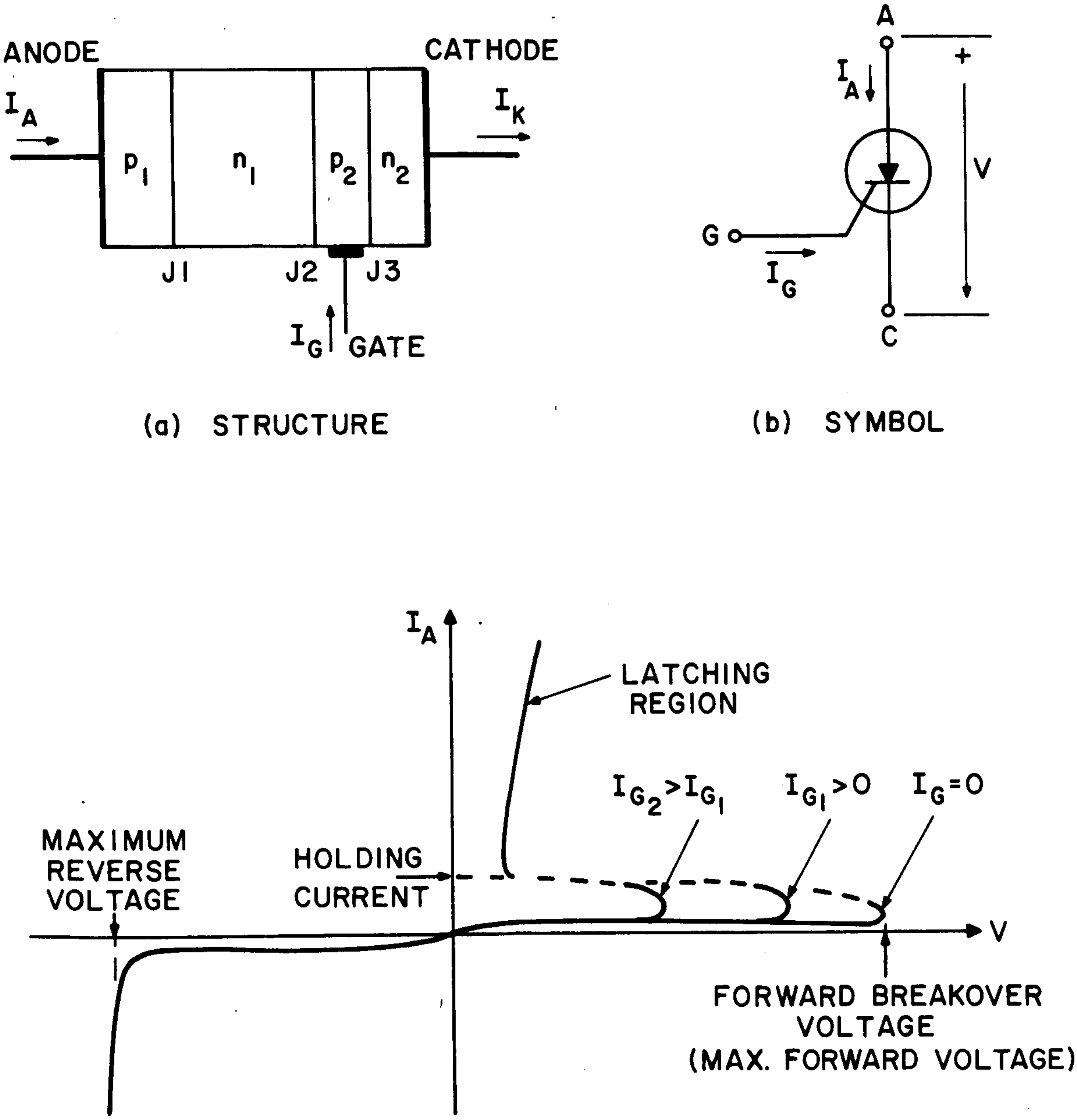

(a) STRUCTURE

(b) SYMBOL

(c) V-I CHARACTERISTICS

FIG. A.1 SCR CHARACTERISTICS

gain is quite low (of the order of 10) and GTO's are forced to operate at much lower current densities than SCR's and so are less economical. Currently available silicon power transistors tend to perform better than the GTO in many applications so that the latter has not received much attention in recent years.

References for Appendix

1. Millman, J. and Taub, H., Pulse, Digital and Switching Waveforms; New York: McGraw-Hill Book Company, 1965; Chapter 12.
2. Bedford, B. D. and Hoft, R. G., Principles of Inverter Circuits; New York: J. Wiley and Sons, 1964; Chapter 1.
3. "Silicon Controlled Rectifier Manual," 4th ed., General Electric Company, Auburn, N.Y., 1967.